

## Electronic Supplementary Information

for

# Reducing the crystallinity of PCL chains by copolymerization with substituted $\delta/\epsilon$ -lactones and its impact on the phase separation of PCL-based block copolymers

Franck Kayser, Guillaume Fleury, Somprasong Thongkham, Christophe Navarro, Blanca Martin-Vaca,\* and Didier Bourissou\*

### Contents

<b>Synthetic procedures and analytical data</b> .....	<b>4</b>
Typical procedure for the preparation of P( $\epsilon$ -CL <sub>21</sub> -co- $\epsilon$ -DL <sub>14</sub> ). .....	4
Typical procedure for the preparation of P( $\epsilon$ -CL <sub>61</sub> -co- $\delta$ -DL <sub>44</sub> ). .....	4
Typical procedure for the preparation of P( $\epsilon$ -CL <sub>96</sub> -co-4-tert-amyl- $\epsilon$ -CL <sub>19</sub> ). .....	5
<b>Tables and Figures</b> .....	<b>6</b>
Table S1. ROP of $\epsilon$ -DL, catalyzed by MSA or HOTf <sup>a</sup> .....	6
Figure S1. Kinetic semilogarithmic plot of ROP of $\epsilon$ -DL .....	6
Figure S2. <sup>1</sup> H NMR (CDCl <sub>3</sub> , 300 MHz) spectrum of P( $\epsilon$ -CL <sub>20</sub> -co- $\epsilon$ -DL <sub>14</sub> ), pentan-1-ol as initiator .....	7
Figure S3. <sup>13</sup> C NMR (CDCl <sub>3</sub> , 300 MHz) spectrum of P( $\epsilon$ -CL <sub>20</sub> -co- $\epsilon$ -DL <sub>14</sub> ), pentan-1-ol as initiator. ....	7
Table S2 : ROP of $\delta$ -DL, catalyzed by MSA or HOTf .....	7
Figure S4. ROP copolymerization of $\delta$ -DL and $\epsilon$ -CL .....	8
Figure S5. ROP copolymerization of $\delta$ -DL and $\epsilon$ -CL .....	8
Figure S6. <sup>1</sup> H NMR (CDCl <sub>3</sub> , 300 MHz) spectrum of P( $\epsilon$ -CL <sub>60</sub> -co- $\delta$ -DL <sub>44</sub> ), pentan-1-ol as initiator. ....	9
Figure S7. <sup>13</sup> C NMR (CDCl <sub>3</sub> , 300 MHz) spectrum of P( $\epsilon$ -CL <sub>60</sub> -co- $\delta$ -DL <sub>44</sub> ), pentan-1-ol as initiator. ....	9
Figure S8. <sup>1</sup> H NMR (CDCl <sub>3</sub> , 300 MHz) spectrum of 4- <i>n</i> -pentyl- $\epsilon$ -CL, 1, in agreement with literature	10
Figure S9. <sup>1</sup> H NMR (CDCl <sub>3</sub> , 300 MHz) of 4- <i>tert</i> -amyl- $\epsilon$ -CL, 2, in agreement with literature .....	10
Figure S10. <sup>1</sup> H NMR (CDCl <sub>3</sub> , 300 MHz) spectrum of 4-Ph- $\epsilon$ -CL, 3, in agreement with literature <sup>1</sup> .....	11
Figure S11. ROP polymerization of 1 (1 mol/L in toluene) catalyzed by MSA .....	11
Figure S12. <sup>1</sup> H NMR (CDCl <sub>3</sub> , 300 MHz) spectrum of P(1), pentan-1-ol as initiator. ....	12
Figure S13. Kinetic semilogarithmic plot of Copolymerization of 1 and $\epsilon$ -CL (1 mol/L in toluene) catalyzed by MSA and initiated by pentan-1-ol with 1/ $\epsilon$ -CL/ $\delta$ -DL/I/MSA = 60/60/1/1. ....	12
Figure S14. <sup>1</sup> H NMR (CDCl <sub>3</sub> , 300 MHz) spectrum of P( $\epsilon$ -CL <sub>110</sub> -co-1 <sub>18</sub> ), benzylic alcohol as initiator. .	13
Figure S15. (a) DSC traces of P( $\epsilon$ -CL <sub>110</sub> -co-1 <sub>18</sub> ) at increasing heating rates .....	13
Figure S16. <sup>1</sup> H NMR (CDCl <sub>3</sub> , 300 MHz) spectrum of P( $\epsilon$ -CL <sub>78</sub> -co-2 <sub>30</sub> ), benzylic alcohol as initiator. ....	14
Figure S17. ROP of 3 (1 mol/L in toluene) catalyzed by MSA and initiated by pentan-1-ol .....	14
Figure S18. <sup>1</sup> H NMR (CDCl <sub>3</sub> , 300 MHz) spectrum of of P(3), pentan-1-ol as initiator. ....	15

Figure S19. $^{13}\text{C}$ NMR ( $\text{CDCl}_3$ , 300 MHz) spectrum of P(3), pentan-1-ol as initiator.....	15
Figure S20. $^{13}\text{C}$ NMR ( $\text{CDCl}_3$ , 300 MHz) spectrum of P( $\epsilon\text{-CL}_{98}\text{-co-3}_{20}$ ), pentan-1-ol as initiator.....	16
Table S3. Values for F, G, H, $\eta$ and $\xi$ calculated from CL and 3 conversion at 30 min. ....	16
Figure S21. Extract of quantitative $^{13}\text{C}$ NMR ( $\text{CDCl}_3$ , 500 MHz) spectra of CL/3 copolymerization ...	17
Figure S22. $^1\text{H}$ NMR ( $\text{CDCl}_3$ , 300 MHz) spectrum of P( $\epsilon\text{-CL}_{98}\text{-co-3}_{20}$ ), pentan-1-ol as initiator. ....	17
Figure S23. Fox plot for the $\epsilon\text{-CL}/3$ copolymers. Dotted red line: theoretical equation.....	18
Figure S24. $^1\text{H}$ NMR spectrum ( $\text{CDCl}_3$ , 300 MHz) of HO-PBD-OH macroinitiator.....	18
Figure S25. $^1\text{H}$ NMR spectrum ( $\text{CDCl}_3$ , 300 MHz) of HO-PBD H-OH macroinitiator. ....	19
Figure S26. $^1\text{H}$ NMR spectrum ( $\text{CDCl}_3$ , 300 MHz) of copolymer PCL <sub>42</sub> - <i>b</i> -PBD- <i>b</i> -PCL <sub>42</sub> .....	19
Figure S27. $^1\text{H}$ NMR spectrum ( $\text{CDCl}_3$ , 300 MHz) of copolymer PCL <sub>80</sub> - <i>b</i> -PBD- <i>b</i> -PCL <sub>80</sub> .....	20
Figure S28. $^1\text{H}$ NMR spectrum ( $\text{CDCl}_3$ , 300 MHz) of copolymer PCL <sub>38</sub> - <i>b</i> -PBD H- <i>b</i> -PCL <sub>38</sub> .....	20
Figure S29. $^1\text{H}$ NMR spectrum ( $\text{CDCl}_3$ , 300 MHz) of copolymer PCL <sub>70</sub> - <i>b</i> -PBD H- <i>b</i> -PCL <sub>70</sub> .....	21
Figure S30. $^1\text{H}$ NMR spectrum ( $\text{CDCl}_3$ , 300 MHz) of copolymer PCL <sub>39</sub> - <i>b</i> -PBD- <i>b</i> -PCL <sub>39</sub> .....	21
Figure S31. $^1\text{H}$ NMR spectrum ( $\text{CDCl}_3$ , 300 MHz) of copolymer PCL <sub>87</sub> - <i>b</i> -PBD- <i>b</i> -PCL <sub>87</sub> .....	22
Figure S32. $^1\text{H}$ NMR spectrum ( $\text{CDCl}_3$ , 300 MHz) of copolymer PCL <sub>am16</sub> - <i>b</i> -PBD H- <i>b</i> -PCL <sub>am16</sub> .....	22
Figure S33. $^1\text{H}$ NMR spectrum ( $\text{CDCl}_3$ , 300 MHz) of copolymer PCL <sub>am35</sub> - <i>b</i> -PBD H- <i>b</i> -PCL <sub>am35</sub> .....	23
Figure S34. $^1\text{H}$ NMR spectrum ( $\text{CDCl}_3$ , 300 MHz) of copolymer PCL <sub>am66</sub> - <i>b</i> -PBD H- <i>b</i> -PCL <sub>am66</sub> .....	23
Figure S35. SEC traces of HO-PBD-OH macroinitiator (blue line) and PCL- <i>b</i> -PBD- <i>b</i> -PCL copolymers (violet, red and green lines).....	24
Figure S36. SEC traces of HO-PBD-OH macroinitiator (blue line) and PCL <sub>am</sub> - <i>b</i> -PBD- <i>b</i> -PCL <sub>am</sub> copolymers (red and green line). ....	24
Figure S37. SEC traces of HO-PBD H-OH macroinitiator (blue line) and PCL- <i>b</i> -PBD- <i>b</i> -PCL copolymers (red and orange line). ....	25
Figure S38. SEC traces of HO-PBD H-OH macroinitiator (blue line) and PCL <sub>am</sub> - <i>b</i> -PBD- <i>b</i> -PCL <sub>am</sub> copolymers (violet, red and orange line). ....	25
Figure S39: 2D DOSY $^1\text{H}$ spectra ( $\delta = 1$ ms and $\Delta = 140$ ms) of $\text{CDCl}_3$ solution of: (a) PBD macroinitiator; (b) P(CL- <i>r</i> -3) of $M_n = 12\,000$ g/mol; (c) BCP PCL <sub>am39</sub> - <i>b</i> -PBD- <i>b</i> -PCL <sub>am39</sub> ; (d) Blend of PBD macroinitiator and P(CL- <i>r</i> -3) .....	26
Figure S40: DSC traces (endo up) obtained for the 2 <sup>nd</sup> heating cycle at 10°C/min for (a) PCL- <i>b</i> -PBD- <i>b</i> -PCL and (b) PCL- <i>b</i> -PBD H- <i>b</i> -PCL, (c) PCL <sub>am</sub> - <i>b</i> -PBD- <i>b</i> -PCL <sub>am</sub> and (d) PCL <sub>am</sub> - <i>b</i> -PBD H- <i>b</i> -PCL <sub>am</sub> triblock copolymers. The curves have been shifted and normalized for clarity. ....	27
Figure S41. Full DSC traces (endo up) obtained at 10°C/min for (a) PCL <sub>80</sub> - <i>b</i> -PBD- <i>b</i> -PCL <sub>80</sub> and (b), PCL <sub>am87</sub> - <i>b</i> -PBD- <i>b</i> -PCL <sub>am87</sub> , (c) PCL <sub>70</sub> - <i>b</i> -PBD H- <i>b</i> -PCL <sub>70</sub> and (d) PCL <sub>am66</sub> - <i>b</i> -PBD H- <i>b</i> -PCL <sub>am66</sub> triblock copolymers. ....	27
Figure S42. TGA traces obtained for selected triblock copolymers: (a) PCL <sub>80</sub> - <i>b</i> -PBD- <i>b</i> -PCL <sub>80</sub> , $T_d = 371$ °C; (b) PCL <sub>am87</sub> - <i>b</i> -PBD- <i>b</i> -PCL <sub>am87</sub> , $T_d = 367$ °C; (c) PCL <sub>70</sub> - <i>b</i> -PBD H- <i>b</i> -PCL <sub>70</sub> , $T_d = 350$ °C; (d) PCL <sub>am66</sub> - <i>b</i> -PBD H- <i>b</i> -PCL <sub>am66</sub> , $T_d = 333$ °C. ....	28
Figure S43. (a) SAXS spectra of PCL- <i>b</i> -PBD- <i>b</i> -PCL and (b) PCL- <i>b</i> -PBD H- <i>b</i> -PCL block copolymers acquired at 100°C. ....	28

Figure S44. (2  $\mu\text{m}$   $\times$  2  $\mu\text{m}$ ) AFM phase images of phase-separated structures obtained for (a) PCL<sub>70</sub>-*b*-PBD H-*b*-PCL<sub>70</sub> and (b) PCL<sub>am66</sub>-*b*-PBD H-*b*-PCL<sub>am66</sub>. .....29

## Synthetic procedures and analytical data

**Typical procedure for the preparation of P( $\epsilon$ -CL<sub>21</sub>-co- $\epsilon$ -DL<sub>14</sub>).**  $\epsilon$ -Caprolactone (192  $\mu$ L, 0.92 mmol, 20 equiv.) and  $\epsilon$ -decalactone (317  $\mu$ L, 0.92 mmol, 20 equiv.) were dissolved in toluene ( $\sum [M]_0 = 1$  mol/L, 3.6 mL). The initiator, *n*-pentanol (5  $\mu$ L, 0.046 mmol, 1 equiv.) and methane sulfonic acid (3  $\mu$ L, 0.046 mmol, 1 equiv.) were successively added. The reaction mixture was stirred at 30 °C. The conversion of the co-monomers was monitored by <sup>1</sup>H NMR spectroscopy. An excess of diisopropylethylamine was added to neutralize the catalyst after 26 hours, and the solvent was evaporated under vacuum. The copolymer was dissolved in a minimum of dichloromethane, precipitated in cold methanol, then filtered and dried under vacuum. Conversion: 70% ( $\epsilon$ -DL) and 99% ( $\epsilon$ -CL); Yield: 80%. SEC (THF):  $M_n = 5\ 100$  g/mol;  $\mathcal{D} = 1.13$ . DSC:  $T_g =$  n.d.;  $T_m =$  n.d. <sup>1</sup>H NMR (CDCl<sub>3</sub>, 300 MHz) : 4.90-4.80 (m, 14×1H, CH<sub>2</sub>CH(CH<sub>2</sub>)O(C=O)), 4.10-4.00 (m, 21×2H, CH<sub>2</sub>O(C=O)), 3.75-3.45 (m, CH<sub>2</sub>OH and CH<sub>2</sub>CH(CH<sub>2</sub>)OH chain end), 2.40-2.20 (m, (21+14)×2H, O(C=O)CH<sub>2</sub>), 1.80-1.20 (m, (14+1)×6H, CH<sub>3</sub>CH<sub>2</sub>CH<sub>2</sub>CH<sub>2</sub>CH<sub>2</sub>O, (21+14)×4H (C=O)CH<sub>2</sub>CH<sub>2</sub>CH<sub>2</sub>CH<sub>2</sub>CH<sub>2</sub>O, (21+14)×2H, COCH<sub>2</sub>CH<sub>2</sub>CH<sub>2</sub>CH<sub>2</sub>CH<sub>2</sub>O), 1.00-0.80 (m, (14+1)×3H, CH<sub>3</sub>CH<sub>2</sub>CH<sub>2</sub>CH<sub>2</sub>CH<sub>2</sub>O).

**Typical procedure for the preparation of P( $\epsilon$ -CL<sub>61</sub>-co- $\delta$ -DL<sub>44</sub>).**  $\epsilon$ -Caprolactone (576  $\mu$ L, 5.52 mmol, 60 equiv.) and  $\delta$ -decalactone (954  $\mu$ L, 5.52 mmol, 60 equiv.) were copolymerized in a minimum of toluene (300  $\mu$ L). The initiator, *n*-pentanol (10  $\mu$ L, 0.092 mmol, 1 equiv.) and methane sulfonic acid (6  $\mu$ L, 0.092 mmol, 1 equiv.) were successively added. The reaction mixture was stirred at 30 °C. The conversion of the co-monomers was monitored by <sup>1</sup>H NMR spectroscopy. An excess of diisopropylethylamine was added to neutralize the catalyst after 42 hours, and the solvent was evaporated under vacuum. The copolymer was dissolved in a minimum of dichloromethane, precipitated in cold methanol (to remove the salts coming from catalyst neutralization), then filtered and dried under vacuum. The copolymer is solubilized in acetone and residual  $\delta$ -decalactone is extracted with an aqueous KOH solution (2 mol/L). The purified copolymer was filtered and dried under vacuum. Conversion: 73% ( $\delta$ -DL) and 99% ( $\epsilon$ -CL); Yield: 75%. SEC (THF):  $M_n = 12\ 500$  g/mol;  $\mathcal{D} = 1.17$ . DSC:  $T_g = -61.1$  °C;  $T_m =$  n.o. <sup>1</sup>H NMR (CDCl<sub>3</sub>, 300 MHz) : 4.90-4.80 (m, 44×1H, CH<sub>2</sub>CH(CH<sub>2</sub>)O(C=O)), 4.10-4.00 (m, 60×2H, CH<sub>2</sub>O(C=O)), 3.75-3.45 (m, CH<sub>2</sub>OH et CH<sub>2</sub>CH(CH<sub>2</sub>)OH chain end), 2.40-2.20 (m, (60+44)×2H, O(C=O)CH<sub>2</sub>), 1.80-1.20 (m, (44+1)×6H, CH<sub>3</sub>CH<sub>2</sub>CH<sub>2</sub>CH<sub>2</sub>CH<sub>2</sub>O, 60×4H COCH<sub>2</sub>CH<sub>2</sub>CH<sub>2</sub>CH<sub>2</sub>CH<sub>2</sub>O, 60×2H, COCH<sub>2</sub>CH<sub>2</sub>CH<sub>2</sub>CH<sub>2</sub>CH<sub>2</sub>O, 44×6H, (C=O)CH<sub>2</sub>CH<sub>2</sub>CH<sub>2</sub>CH(CH<sub>2</sub>)O), 1.00-0.80 (m, 44×3H, CH<sub>3</sub>CH<sub>2</sub>CH<sub>2</sub>CH<sub>2</sub>O et 3H, CH<sub>3</sub>CH<sub>2</sub>CH<sub>2</sub>CH<sub>2</sub>CH<sub>2</sub>O).

**Typical procedure for the preparation of P( $\epsilon$ -CL<sub>84</sub>-co-4-*n*-pentyl- $\epsilon$ -CL<sub>42</sub>).**  $\epsilon$ -Caprolactone (430 mg, 3.77 mmol, 78 equiv.) and 4-*n*-pentyl- $\epsilon$ -caprolactone (410 mg, 2.03 mmol, 42 equiv.) were dissolved in toluene ( $\sum [M]_0 = 1$  mol/L, 5.7 mL). The initiator, benzyl alcohol (5  $\mu$ L, 0.048 mmol,

1 equiv.) and methane sulfonic acid (3  $\mu$ L, 0.048 mmol, 1 equiv.) were successively added. The reaction mixture was stirred at 30 °C. The conversion of the co-monomers was monitored by  $^1\text{H}$  NMR spectroscopy. An excess of diisopropylethylamine was added to neutralize the catalyst after 7.5 h, and the solvent was evaporated under vacuum. The copolymer was dissolved in a minimum of dichloromethane, precipitated in cold methanol, then filtered and dried under vacuum. Conversion: 99% (4-*n*-pentyl- $\epsilon$ -CL) and 99% ( $\epsilon$ -CL) Yield: 90%. SEC (THF):  $M_n$  = 16 800 g/mol;  $\mathcal{D}$  = 1.15. DSC:  $T_g$  = -67.2 °C;  $T_m$  = n.o.  $^1\text{H}$  NMR (CDCl<sub>3</sub>, 300 MHz): 7.35-7.28 (m, 5H, PhCH<sub>2</sub>O), 5.15-5.00 (m, 2H, PhCH<sub>2</sub>O), 4.15-3.90 (m, (84+42)×2H, CH<sub>2</sub>O(C=O)), 3.75-3.55 (m, CH<sub>2</sub>OH chain end), 2.45-2.20 (m, (84+42)×2H, O(C=O)CH<sub>2</sub>), 1.80-1.20 (m, 42×8H, CH<sub>3</sub>CH<sub>2</sub>CH<sub>2</sub>CH<sub>2</sub>CH<sub>2</sub>CH<sub>2</sub>CH, 84×4H (C=O)CH<sub>2</sub>CH<sub>2</sub>CH<sub>2</sub>CH<sub>2</sub>CH<sub>2</sub>O, 42×4H (C=O)CH<sub>2</sub>CH<sub>2</sub>CH(pentyl)CH<sub>2</sub>CH<sub>2</sub>O, 84×2H (C=O)CH<sub>2</sub>CH<sub>2</sub>CH<sub>2</sub>CH<sub>2</sub>CH<sub>2</sub>O, 42×1H (C=O)CH<sub>2</sub>CH<sub>2</sub>CH(pentyl)CH<sub>2</sub>CH<sub>2</sub>O), 1.00-0.80 (m, 42×3H, CH<sub>3</sub>CH<sub>2</sub>CH<sub>2</sub>CH<sub>2</sub>CH<sub>2</sub>CH).

**Typical procedure for the preparation of P( $\epsilon$ -CL<sub>96</sub>-*co*-4-*tert*-amyl- $\epsilon$ -CL<sub>19</sub>).**  $\epsilon$ -Caprolactone (480 mg, 4.64 mmol, 96 equiv.) and 4-*tert*-amyl- $\epsilon$ -caprolactone (194 mg, 1.16 mmol, 24 equiv.) were dissolved in toluene ( $\sum [M]_0 = 1$  mol/L, 5.7 mL). The initiator, benzyl alcohol (5  $\mu$ L, 0.048 mmol, 1 equiv.) and methane sulfonic acid (3  $\mu$ L, 0.048 mmol, 1 equiv.) were successively added. The reaction mixture was stirred at 30 °C. The conversion of the co-monomers was monitored by  $^1\text{H}$  NMR spectroscopy. An excess of diisopropylethylamine was added to neutralize the catalyst after 4 hours and half, and the solvent was evaporated under vacuum. The copolymer was dissolved in a minimum of dichloromethane, precipitated in cold methanol, then filtered and dried under vacuum. Conversion: 70% (4-*tert*-pentyl- $\epsilon$ -CL) and 99% ( $\epsilon$ -CL); Yield: 75%. SEC (THF):  $M_n$  = 11 700 g/mol;  $\mathcal{D}$  = 1.10. DSC:  $T_g$  = -59.3 °C;  $T_m$  = 34.6 °C.  $^1\text{H}$  NMR (CDCl<sub>3</sub>, 300 MHz): 7.35-7.28 (m, 5H, PhCH<sub>2</sub>O), 5.10-5.00 (m, 2H, PhCH<sub>2</sub>O), 4.15-3.90 (m, (96+19)×2H, CH<sub>2</sub>O(C=O)), 3.75-3.55 (m, CH<sub>2</sub>OH chain end), 2.45-2.20 (m, (96+19)×2H, O(C=O)CH<sub>2</sub>), 2.00-1.80 (m, 19×2H, CH<sub>2</sub>CH(*tert*-amyl)CH<sub>2</sub>CH<sub>2</sub>O), 1.80-1.50 (m, 96×4H, (C=O)CH<sub>2</sub>CH<sub>2</sub>CH<sub>2</sub>CH<sub>2</sub>CH<sub>2</sub>O), 1.50-1.25 (m, 96×2H, COCH<sub>2</sub>CH<sub>2</sub>CH<sub>2</sub>CH<sub>2</sub>CH<sub>2</sub>O, 19×2H, (C=O)CH<sub>2</sub>CH<sub>2</sub>CH(*tert*-amyl)CH<sub>2</sub>CH<sub>2</sub>O, 19×2H, CHC(CH<sub>3</sub>)<sub>2</sub>CH<sub>2</sub>CH<sub>3</sub>), 1.15-1.00 (m, 19×1H, (C=O)CH<sub>2</sub>CH<sub>2</sub>CH(*tert*-amyl)CH<sub>2</sub>CH<sub>2</sub>O), 0.90-0.75 (m, 19×2×3H, CHC(CH<sub>3</sub>)<sub>2</sub>CH<sub>2</sub>CH<sub>3</sub>, 19×3H, CHC(CH<sub>3</sub>)<sub>2</sub>CH<sub>2</sub>CH<sub>3</sub>).

## Tables and Figures

**Table S1.** ROP of  $\epsilon$ -DL, catalyzed by MSA or HOTf<sup>a</sup>

Entry	Catalyst	Conditions	T (°C)	Time (h)	Conversion ( <sup>1</sup> H NMR)	DP <sub>NMR</sub>	M <sub>nSEC</sub> <sup>c</sup> (g/mol)	D <sup>c</sup>
1	HOTf <sup>b</sup>	4 mol/L	30	21	0.91	17	1 000	1.70
2	MSA <sup>a</sup>	1 mol/L	30	74	0.91	28	5 000	1.20
3	MSA <sup>a</sup>	4 mol/L	30	74	0.90	30	6 800	1.12
4	MSA <sup>a</sup>	Bulk	30	71	0.76	22	3 100	1.27
5	MSA <sup>a</sup>	4 mol/L	50	30	0.92	34	3 400	1.34
6	MSA <sup>a</sup>	4 mol/L	80	28	0.78	29	2 800	1.43
7	MSA <sup>b</sup>	4 mol/L	30	28	0.93	28	3 100	1.40

<sup>a</sup> Typical polymerization conditions: M/I/cat.= 40/1/1; <sup>b</sup> M/I/cat.= 40/1/3. <sup>c</sup> Determined by SEC in THF using PS standards

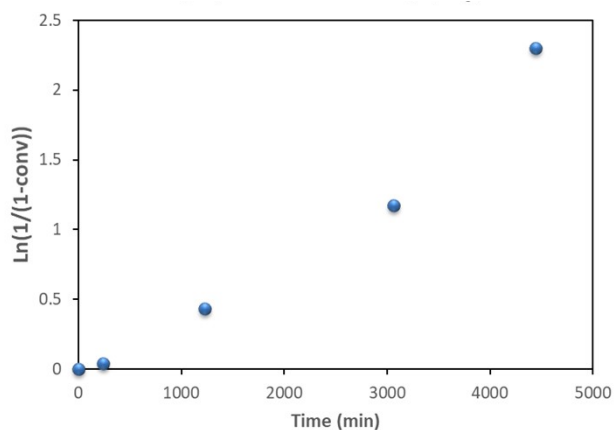


**Figure S1.** Kinetic semilogarithmic plot of ROP of  $\epsilon$ -DL (toluene,  $[\epsilon\text{-DL}]_0 = 4 \text{ mol/L}$ ) catalyzed by MSA and initiated by pentan-1-ol with  $\epsilon\text{-DL/I/MSA} = 40/1/1$  at 30 °C.

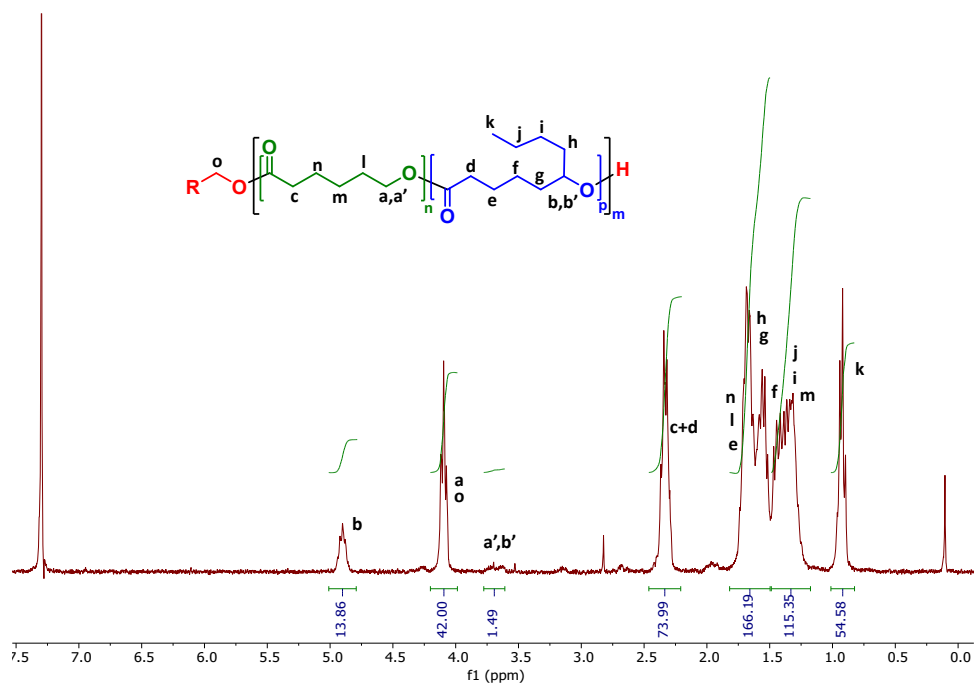


Figure S2. <sup>1</sup>H NMR (CDCl<sub>3</sub>, 300 MHz) spectrum of P(ε-CL<sub>20</sub>-co-ε-DL<sub>14</sub>), pentan-1-ol as initiator.

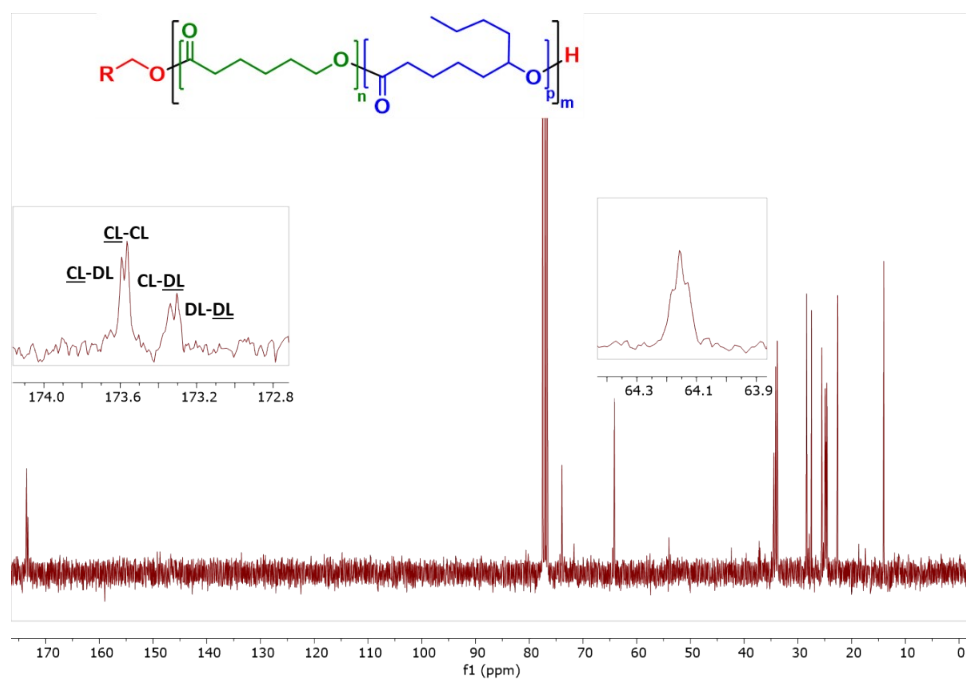
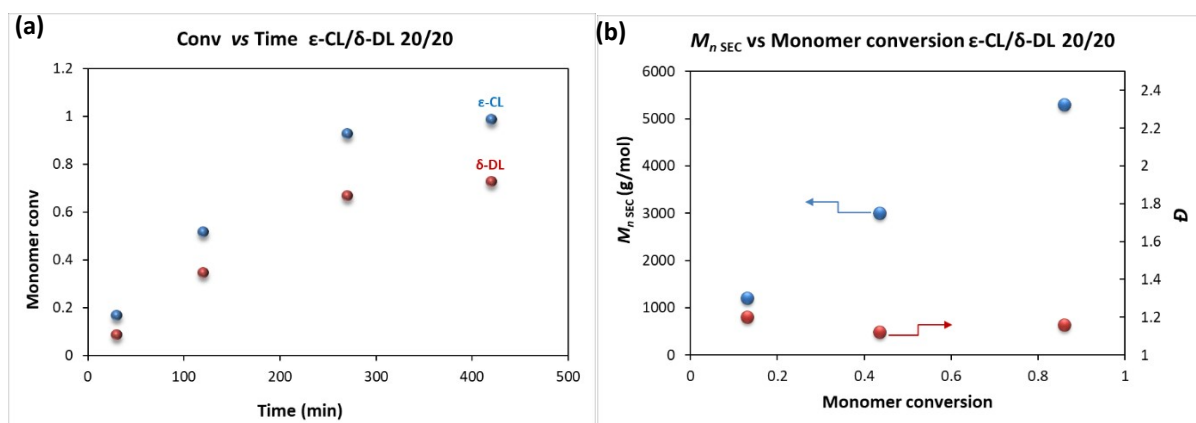


Figure S3. <sup>13</sup>C NMR (CDCl<sub>3</sub>, 300 MHz) spectrum of P(ε-CL<sub>20</sub>-co-ε-DL<sub>14</sub>), pentan-1-ol as initiator.

Table S2 : ROP of δ-DL, catalyzed by MSA or HOTf<sup>a</sup>

Run	Catalyst	[δ-DL] <sub>0</sub>	Time (h)	Conversion <sub>NMR</sub>	DP <sub>NMR</sub> <sup>b</sup>	M <sub>n</sub> (g/mol) <sup>c</sup>	D <sup>c</sup>
1	MSA	1 mol/L	48	0.12	5	1 500	1.16
2	MSA	4 mol/L	23	0.74	17	3 200	1.31
3	MSA	bulk	18	0.81	26	6 100	1.13
4	HOTf	bulk	22	0.81	26	5 000	1.22

<sup>a</sup> Reaction conditions: M/I/cat.: 40/1/1; 30 °C. <sup>b</sup> Determined by <sup>1</sup>H NMR spectroscopy. <sup>c</sup> Determined by SEC using PS standards.



**Figure S4.** ROP copolymerization of  $\delta$ -DL and  $\epsilon$ -CL (in bulk) catalyzed by MSA and initiated by pentan-1-ol with  $\epsilon$ -CL/ $\delta$ -DL/I/MSA = 20/20/1/1 at 30 °C (a) Kinetic semilogarithmic plot and (b)  $M_{n,SEC}$  vs total monomer conversion plot.

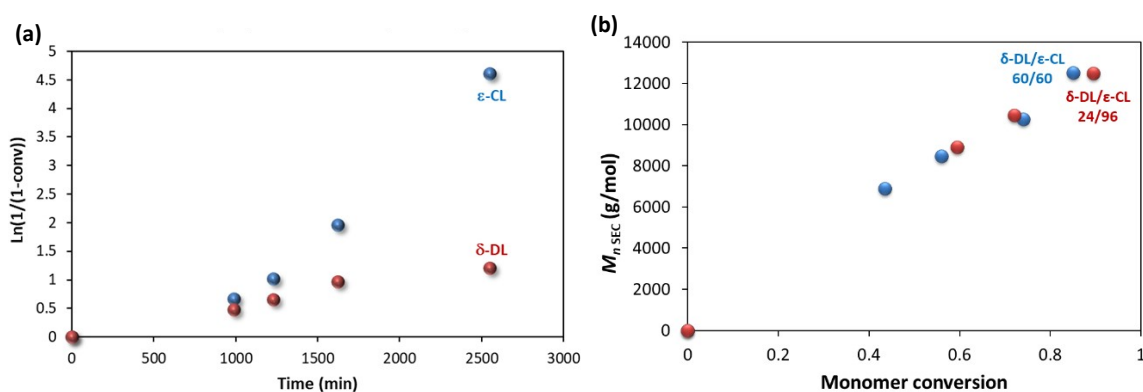


**Figure S5.** ROP copolymerization of  $\delta$ -DL and  $\epsilon$ -CL (25% vol toluene) catalyzed by MSA and initiated by pentan-1-ol with  $\epsilon$ -CL/ $\delta$ -DL/I/MSA = 60/60/1/1 at 30 °C (a) Kinetic semilogarithmic plot and (b)  $M_{n,SEC}$  vs total monomer conversion plot.



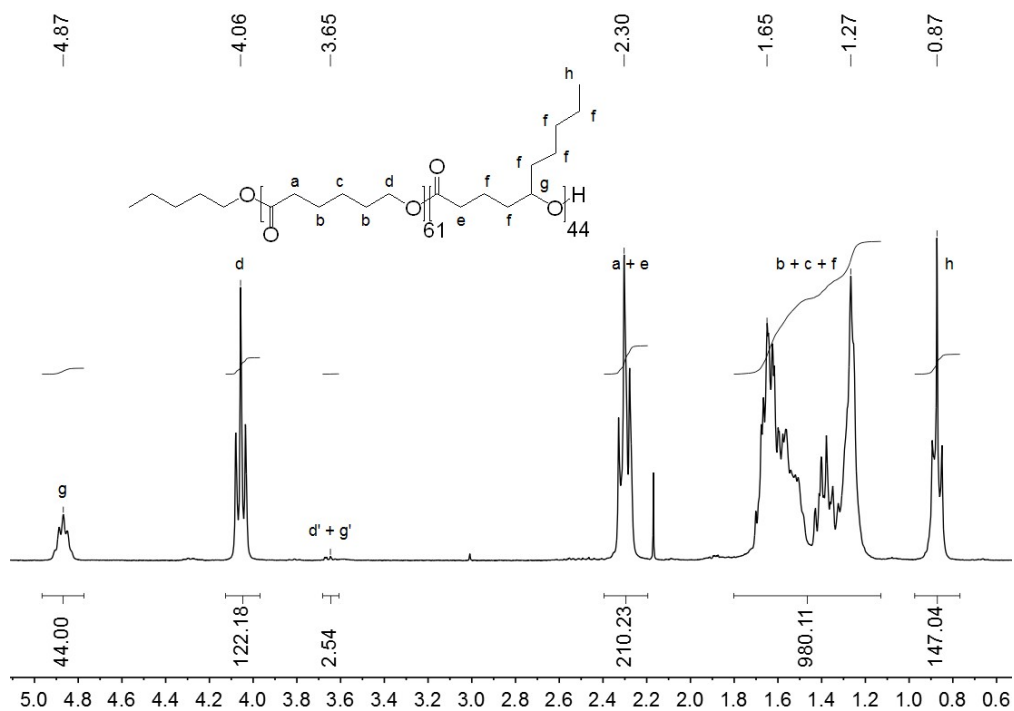


**Figure S6.** <sup>1</sup>H NMR (CDCl<sub>3</sub>, 300 MHz) spectrum of P(ε-CL<sub>60</sub>-co-δ-DL<sub>44</sub>), pentan-1-ol as initiator.

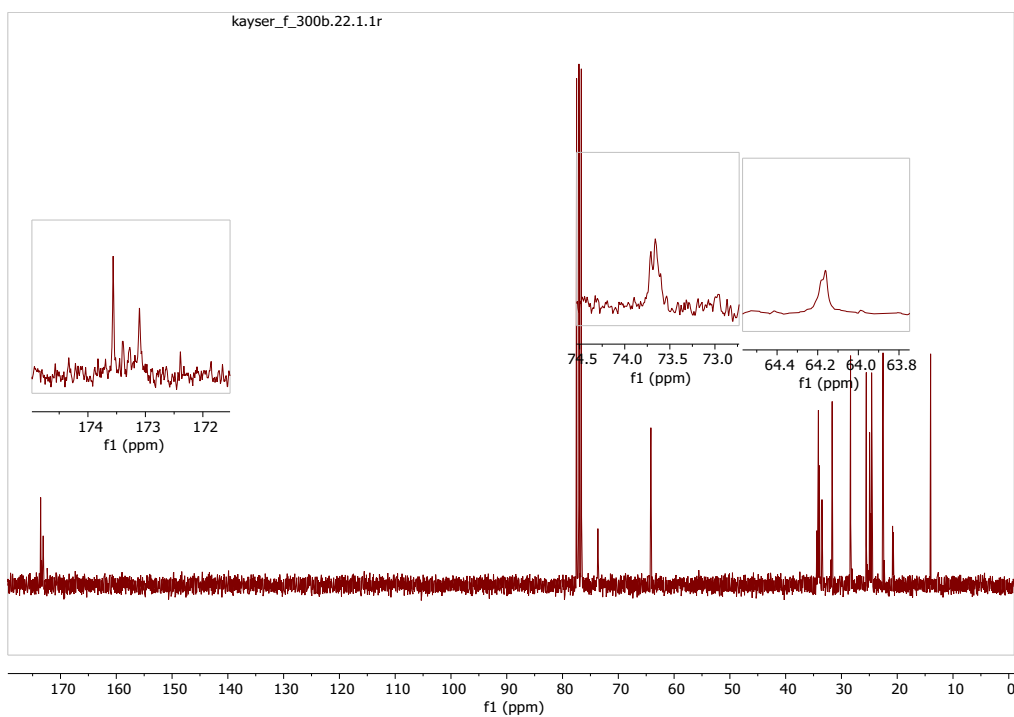


**Figure S7.** <sup>13</sup>C NMR (CDCl<sub>3</sub>, 300 MHz) spectrum of P(ε-CL<sub>60</sub>-co-δ-DL<sub>44</sub>), pentan-1-ol as initiator.

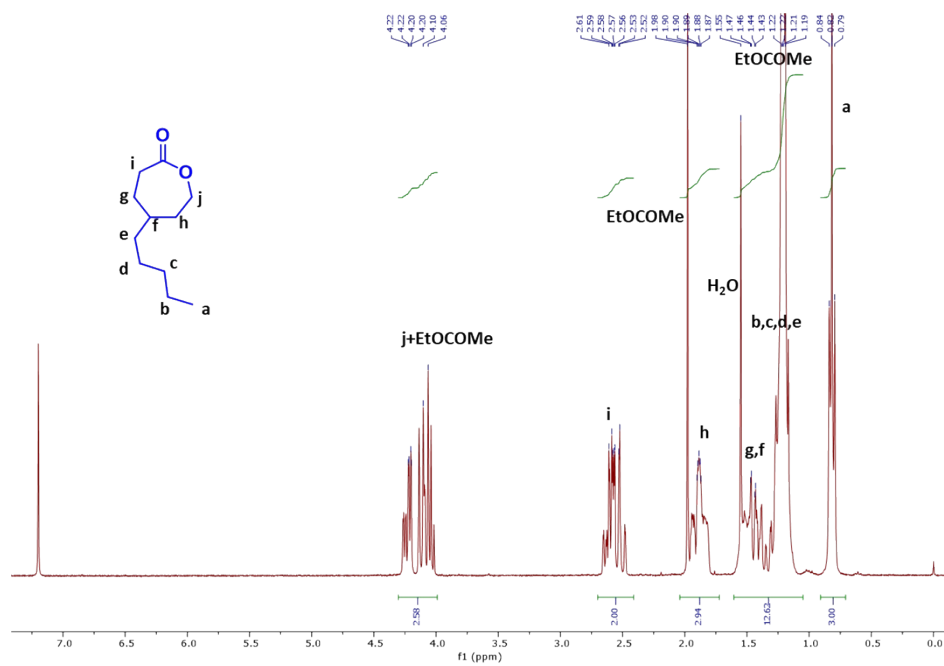


**Figure S8.**  $^1\text{H}$  NMR (CDCl<sub>3</sub>, 300 MHz) spectrum of 4-*n*-pentyl- $\epsilon$ -CL, **1**, in agreement with literature<sup>1</sup>

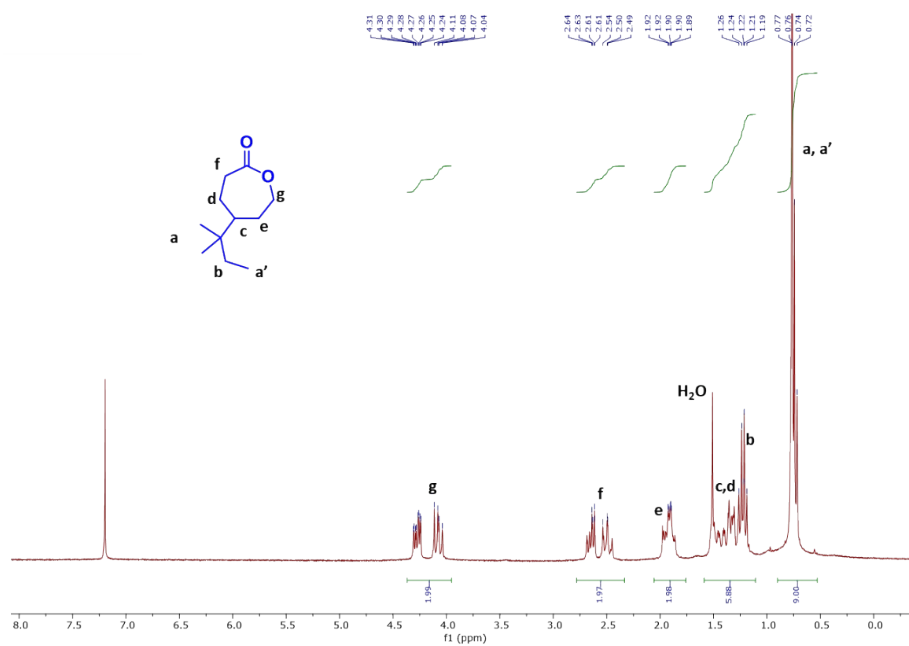


**Figure S9.**  $^1\text{H}$  NMR (CDCl<sub>3</sub>, 300 MHz) of 4-*tert*-amyl- $\epsilon$ -CL, **2**, in agreement with literature<sup>2</sup>

<sup>1</sup> Leisch, H.; Shi, R.; Grosse, S.; Morley, K.; Bergeron, H.; Cygler, M.; Iwaki, H.; Hasegawa, Y.; Lau, P. C. K. *Appl. Environ. Microbiol.* **2012**, *78* (7), 2200–2212.

<sup>2</sup> Klok, H.-A.; Becker, S.; Schuch, F.; Pakula, T.; Müllen, K. *Macromol. Biosci.* **2003**, *3* (12), 729–741.

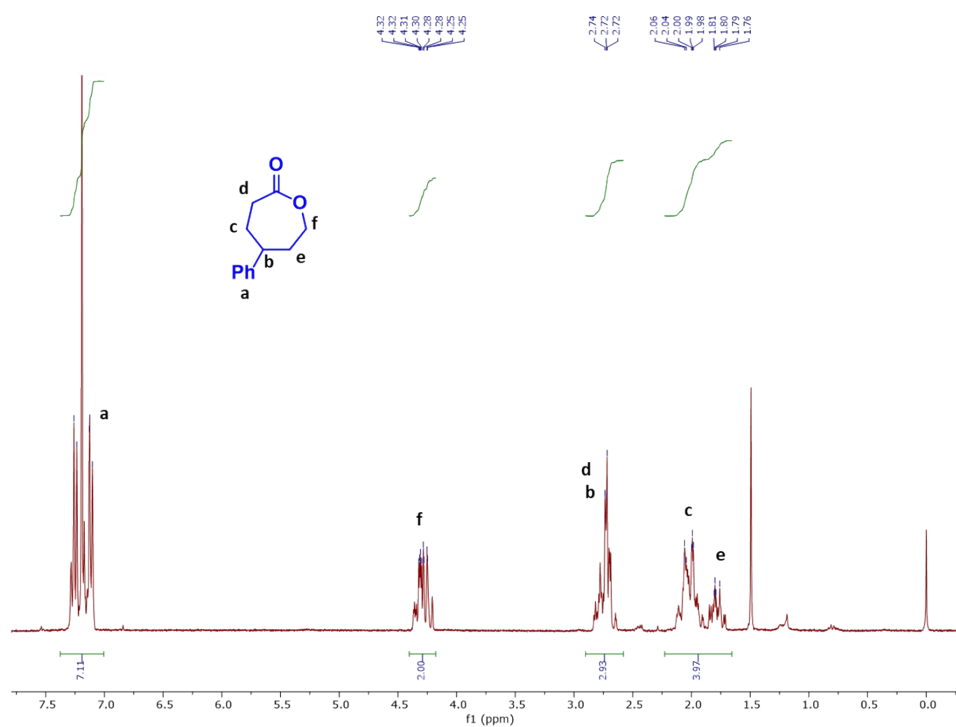


**Figure S10.**  $^1\text{H}$  NMR ( $\text{CDCl}_3$ , 300 MHz) spectrum of 4-Ph- $\epsilon$ -CL, **3**, in agreement with literature<sup>1</sup>

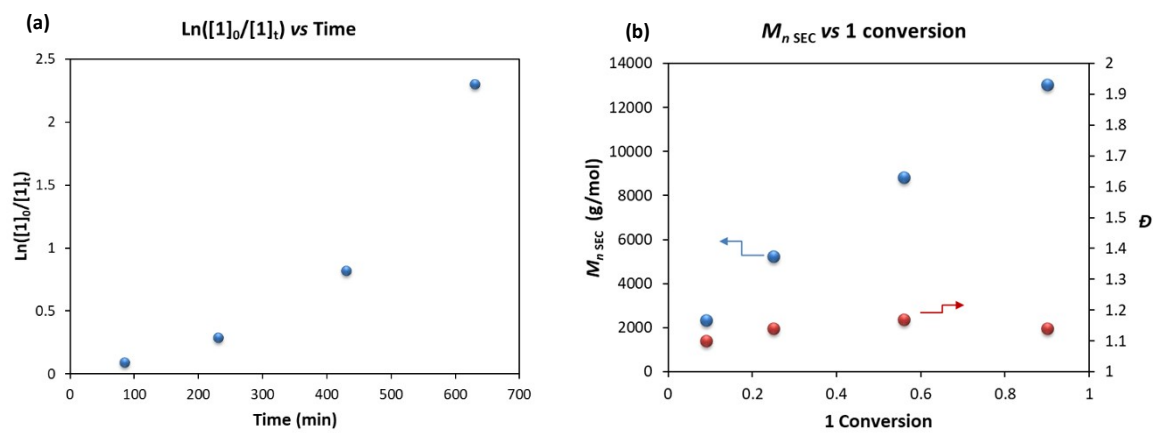


**Figure S11.** ROP polymerization of **1** (1 mol/L in toluene) catalyzed by MSA and initiated by pentan-1-ol with  $1/\text{I}/\text{MSA} = 120/1/1$  at 30 °C (a) Kinetic semilogarithmic plot and (b)  $M_{n,\text{SEC}}$  vs total monomer conversion plot.

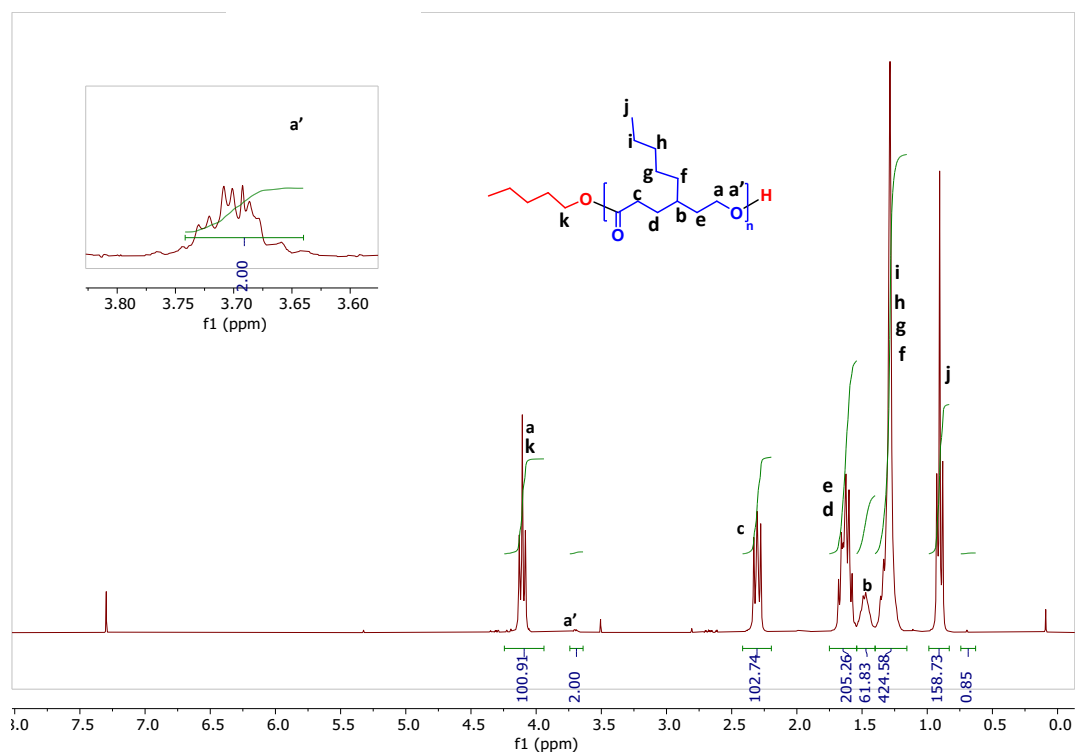


**Figure S12.** <sup>1</sup>H NMR (CDCl<sub>3</sub>, 300 MHz) spectrum of P(1), pentan-1-ol as initiator.

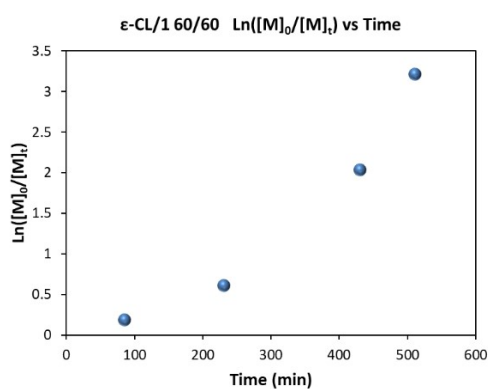


**Figure S13.** Kinetic semilogarithmic plot of Copolymerization of **1** and ε-CL (1 mol/L in toluene) catalyzed by MSA and initiated by pentan-1-ol with **1**/ε-CL/δ-DL/I/MSA = 60/60/1/1.

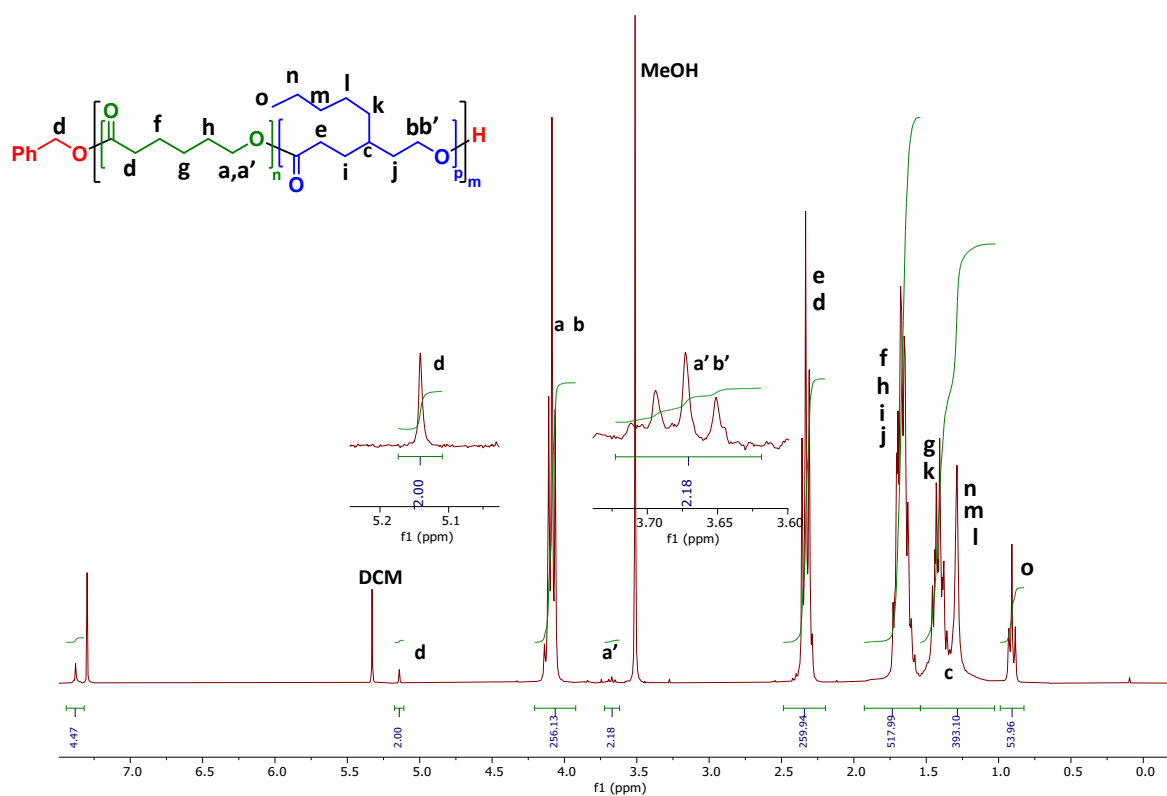


Figure S14.  $^1\text{H}$  NMR ( $\text{CDCl}_3$ , 300 MHz) spectrum of  $\text{P}(\epsilon\text{-CL}_{110}\text{-co-1}_{18})$ , benzylic alcohol as initiator.

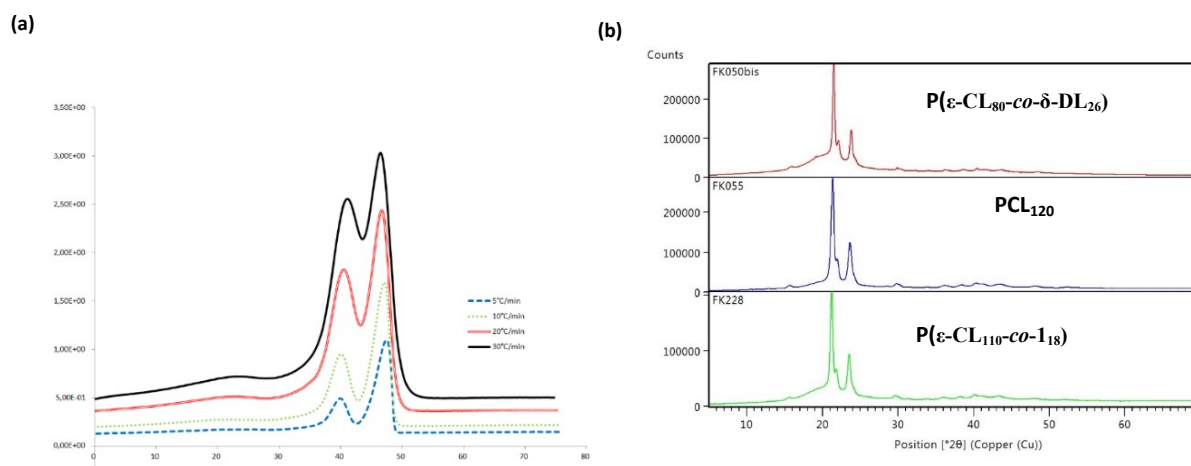
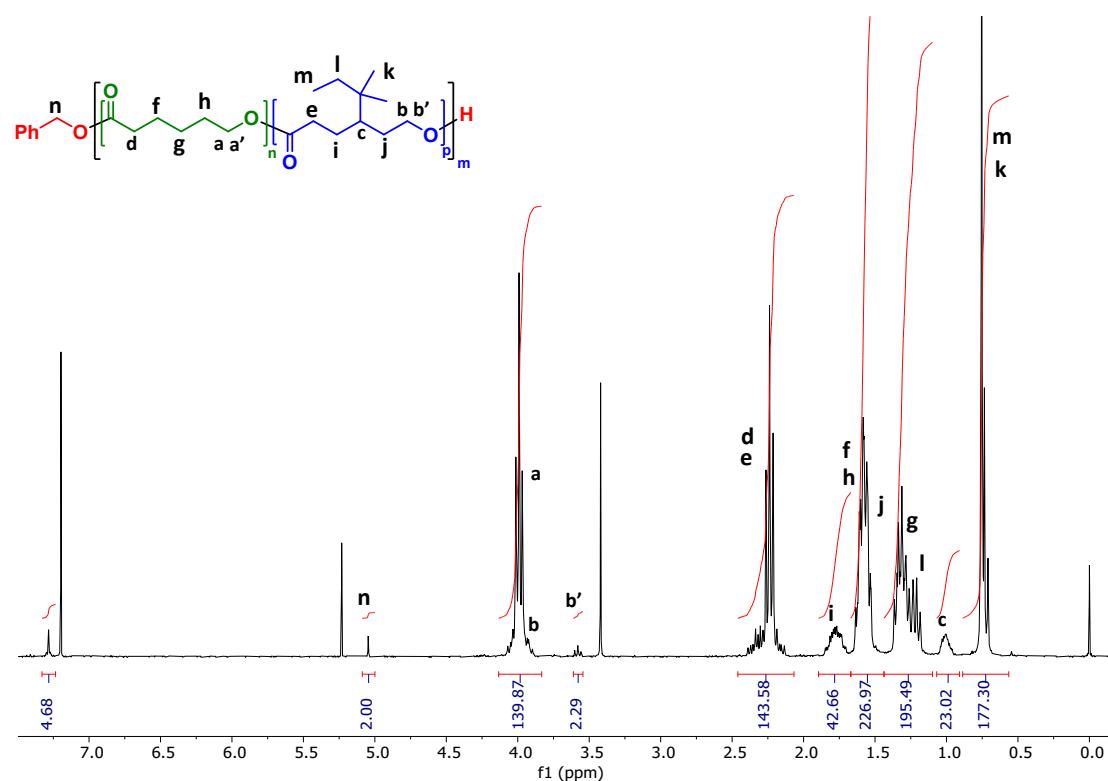
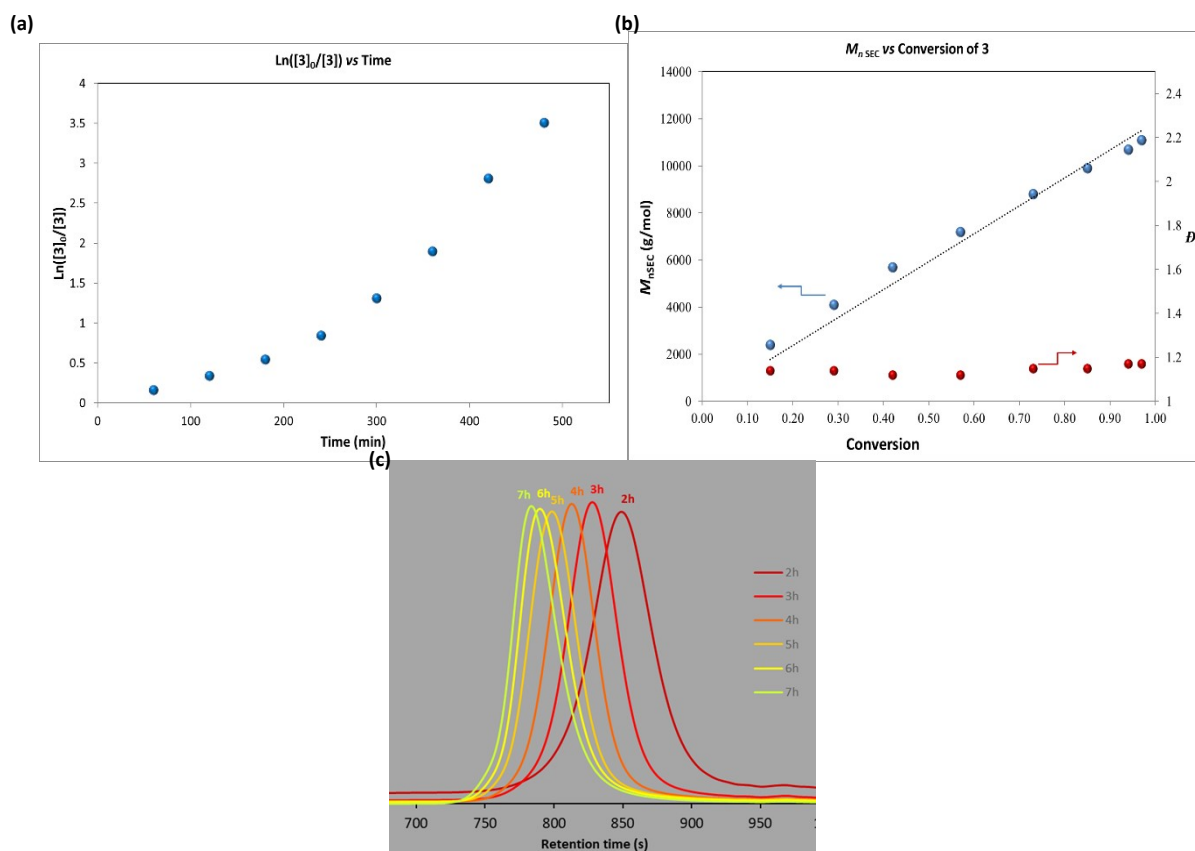


Figure S15. (a) DSC traces of  $\text{P}(\epsilon\text{-CL}_{110}\text{-co-1}_{18})$  at increasing heating rates, and (b) Powder DRX of 3 polymer samples  $\text{P}(\epsilon\text{-CL}_{80}\text{-co-}\delta\text{-DL}_{26})$  (top),  $\text{PCL}_{120}$  (middle), and  $\text{P}(\epsilon\text{-CL}_{110}\text{-co-1}_{18})$  (bottom).



**Figure S16.** <sup>1</sup>H NMR (CDCl<sub>3</sub>, 300 MHz) spectrum of P(ε-CL<sub>78</sub>-co-2<sub>30</sub>), benzylic alcohol as initiator.



**Figure S17.** ROP of **3** (1 mol/L in toluene) catalyzed by MSA and initiated by pentan-1-ol with 3/I/MSA = 60/1/1 at 30 °C: (a) Kinetic semilogarithmic plot, (b)  $M_{n,SEC}$  vs total monomer conversion plot and (c) SEC traces

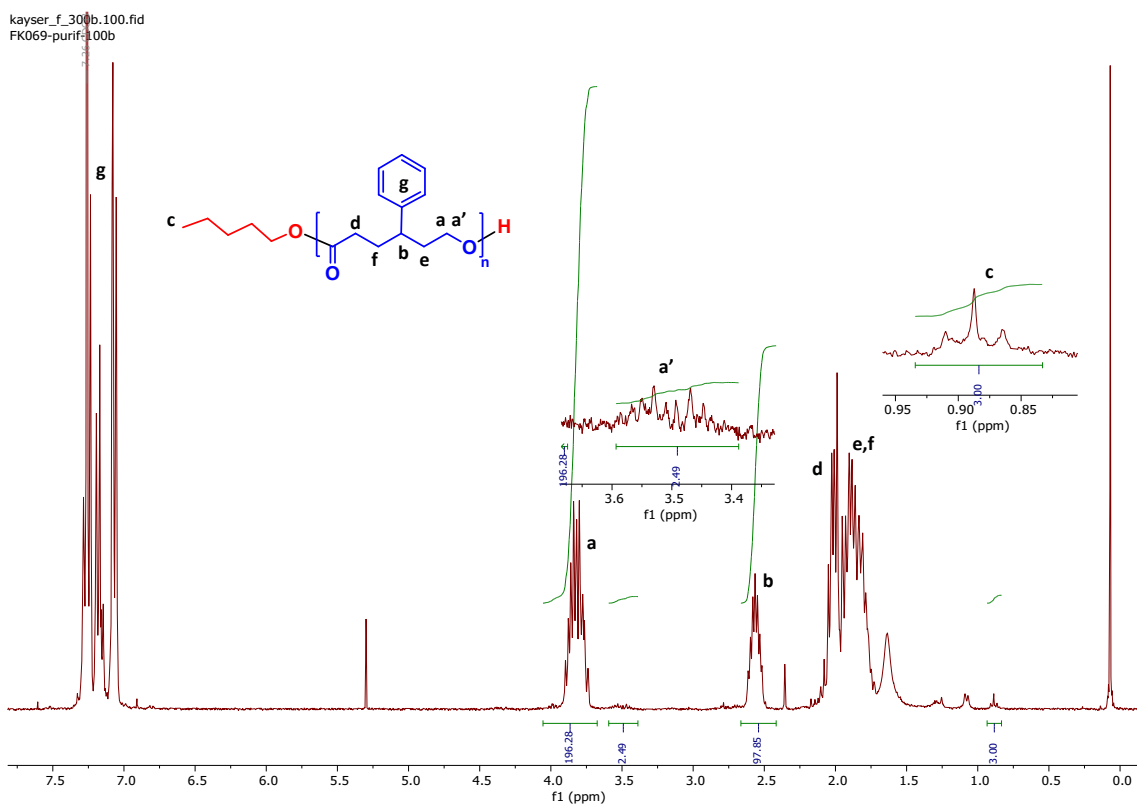


**Figure S18.** <sup>1</sup>H NMR (CDCl<sub>3</sub>, 300 MHz) spectrum of P(3), pentan-1-ol as initiator.

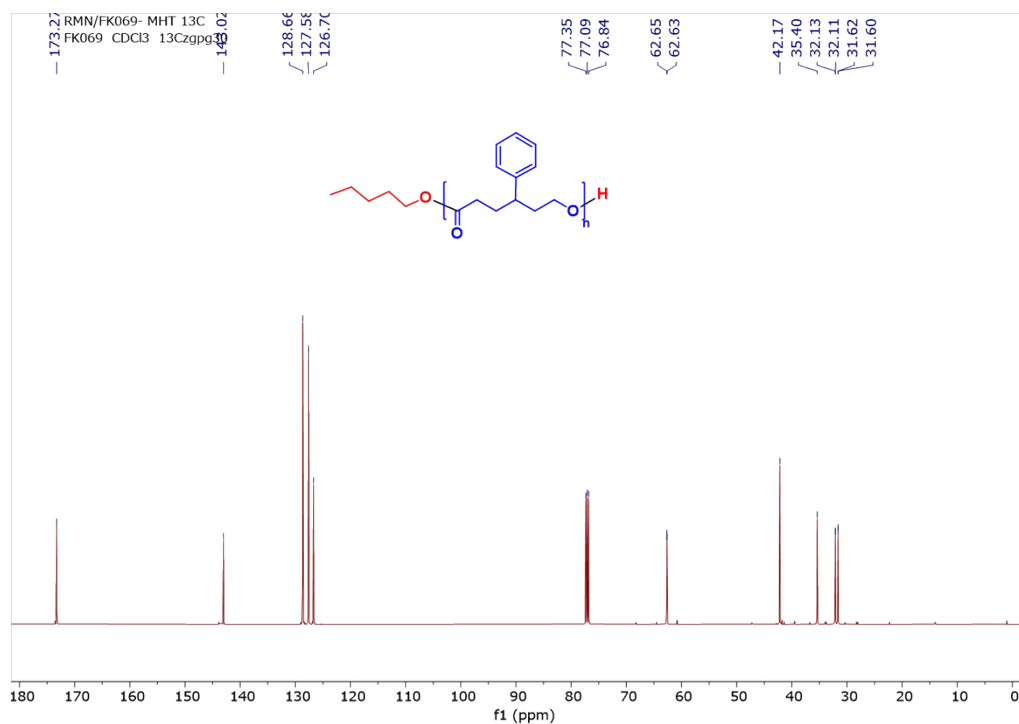


**Figure S19.** <sup>13</sup>C NMR (CDCl<sub>3</sub>, 300 MHz) spectrum of P(3), pentan-1-ol as initiator.

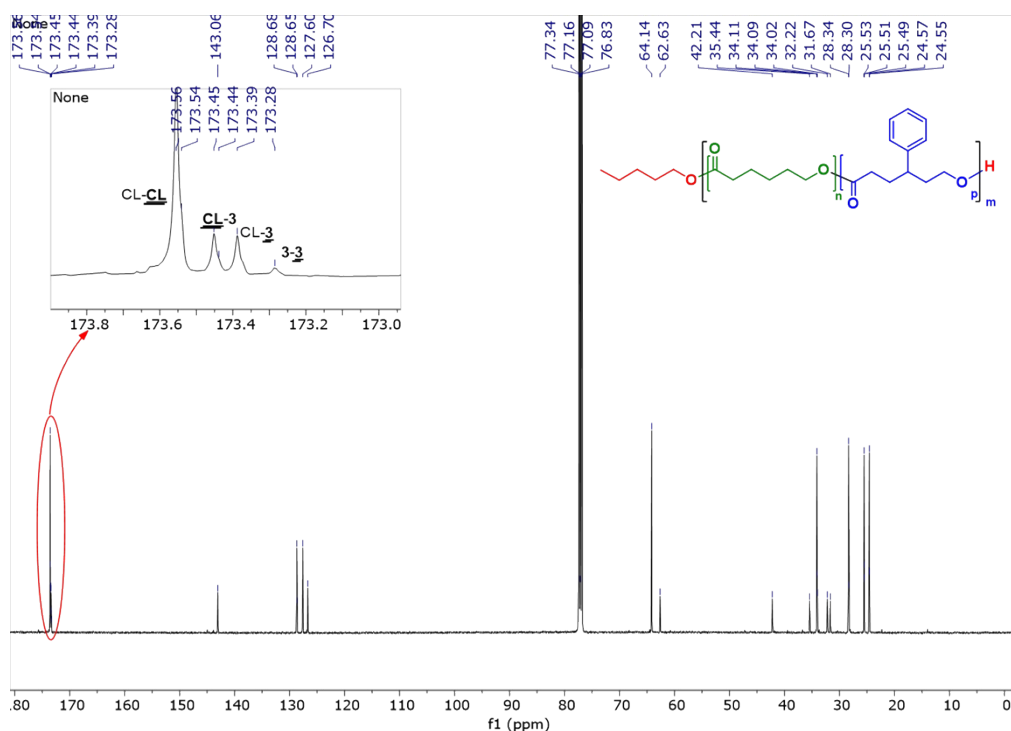


**Figure S20.**  $^{13}\text{C}$  NMR ( $\text{CDCl}_3$ , 300 MHz) spectrum of  $\text{P}(\epsilon\text{-CL}_{98}\text{-co-}\mathbf{3}_{20})$ , pentan-1-ol as initiator.

In order to determine the reactivity ratios according to the Kelen-Tüdös method, it is necessary to know the composition of the reaction medium in comonomer, as well as the exact composition of the copolymer formed, by varying the proportions of comonomers in separate copolymerizations. It is important that the copolymerization are stopped before reaching a high conversion. Ideally the conversion should be less than 10%.

Starting from Mayo-Lewis<sup>3</sup> equation and applying Kelen-Tüdös<sup>4</sup> method, the monomers reactivity ratios have been determined from the curve  $\eta = f(\xi)$  by studying co-monomers conversion by quantitative  $^{13}\text{C}$  NMR analysis.

**Table S3.** Values for F, G, H,  $\eta$  and  $\xi$  calculated from CL and **3** conversion at 30 min.

$\epsilon\text{-CL}/4\text{-Ph-}\epsilon\text{-CL}$ feed ratio	$\epsilon\text{-CL}$ Conv *	<b>3</b> Conv*	F	G	H <sup>o</sup>	$\eta$	$\xi^o$
96/24	9.5	12.5	5.02	2.36	0.40	0.40	0.84
72/48	6.7	6.3	1.29	0.47	0.21	0.21	0.58
48/72	9.1	7.9	0.53	-0.21	-0.15	-0.15	0.37
24/96	10.5	8.2	0.17	-0.54	-0.49	-0.49	0.16

\* Determined by quantitative  $^{13}\text{C}$  NMR ( $\text{CDCl}_3$ , 500 MHz); <sup>o</sup> Calculated with  $\alpha = 0.93$

<sup>3</sup> Mayo, F. R.; Lewis, F. M. *J. Am. Chem. Soc.* **1944**, 66 (9), 1594–1601.

<sup>4</sup> a) Kelen, T.; Tüdös, F. *J. Macromol. Sci. Part - Chem.* **1975**, 9 (1), 1–27. b) Tüdös, F.; Kelen, T. *J. Macromol. Sci. Part - Chem.* **1981**, 16 (7), 1283–1297.



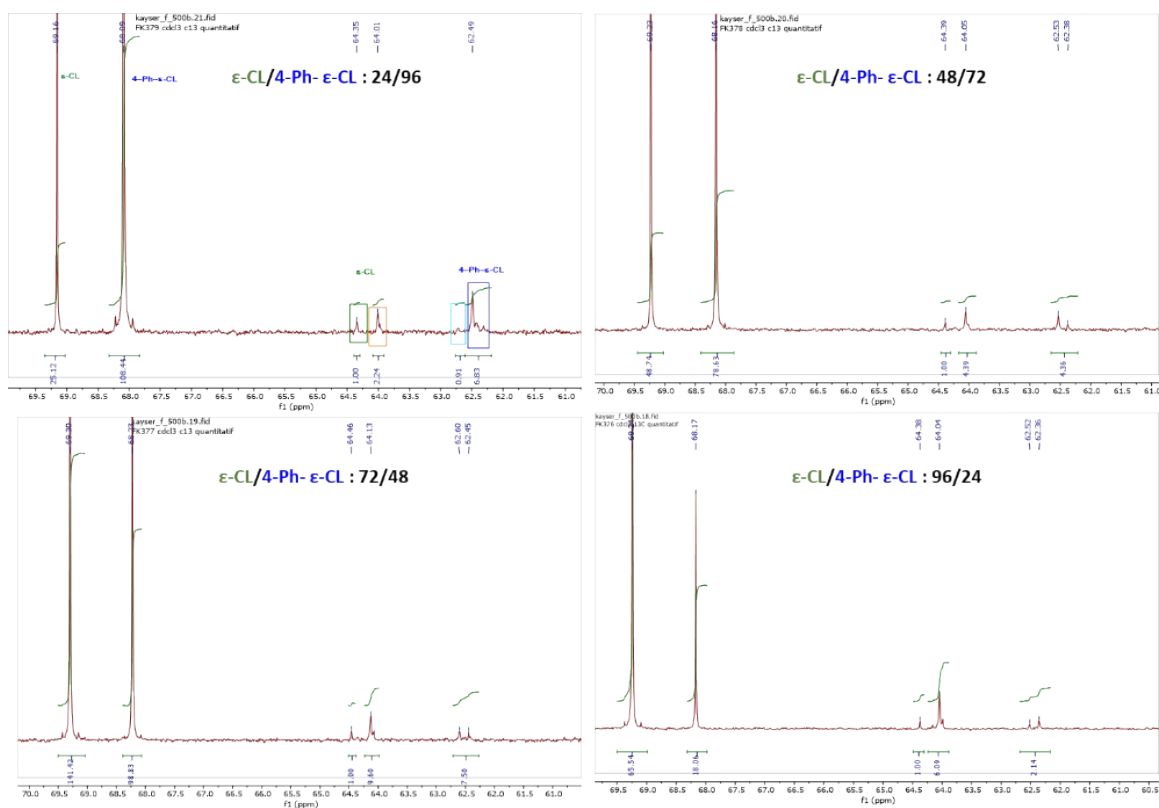


**Figure S21.** Extract of quantitative  $^{13}\text{C}$  NMR ( $\text{CDCl}_3$ , 500 MHz) spectra of CL/**3** copolymerization at different monomer ratios for monomer conversions less than 10%.

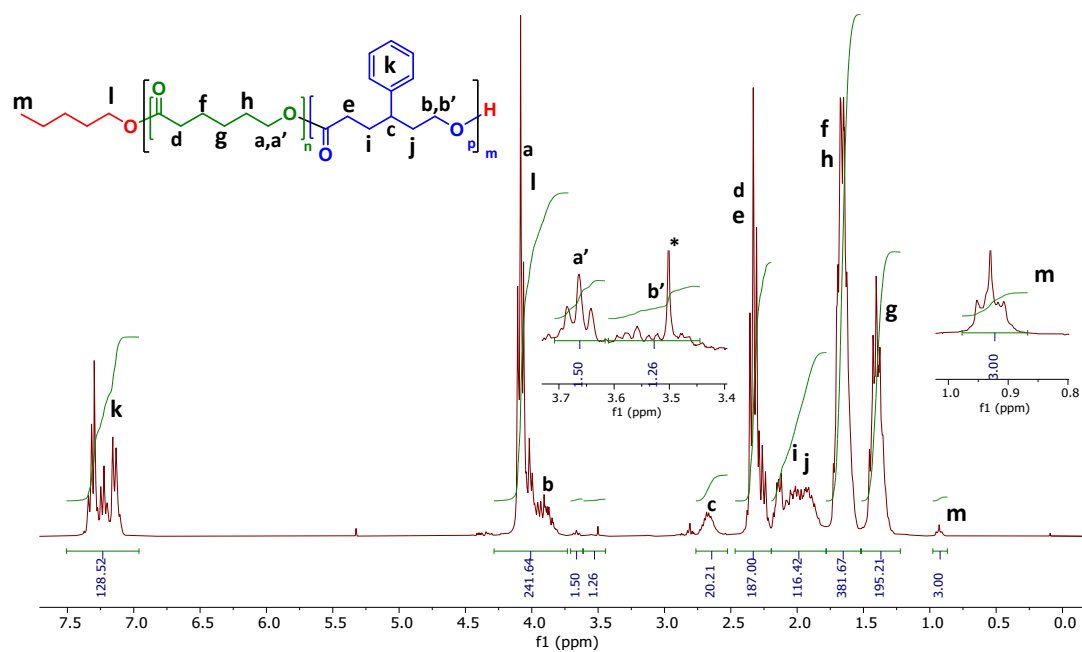


**Figure S22.**  $^1\text{H}$  NMR ( $\text{CDCl}_3$ , 300 MHz) spectrum of  $\text{P}(\epsilon\text{-CL}_{98}\text{-co-}\mathbf{3}_{20})$ , pentan-1-ol as initiator.

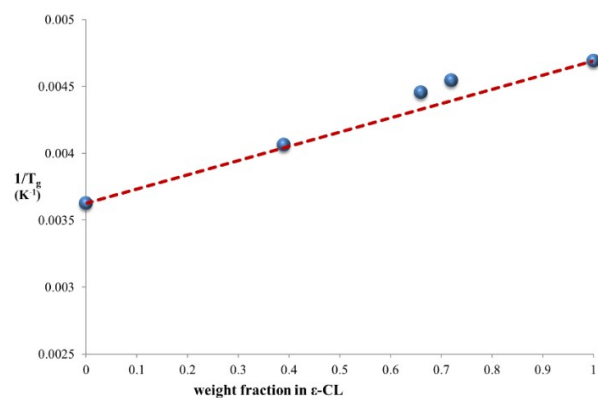


**Figure S23.** Fox plot for the  $\epsilon$ -CL/3 copolymers. Doted red line: theoretical equation.

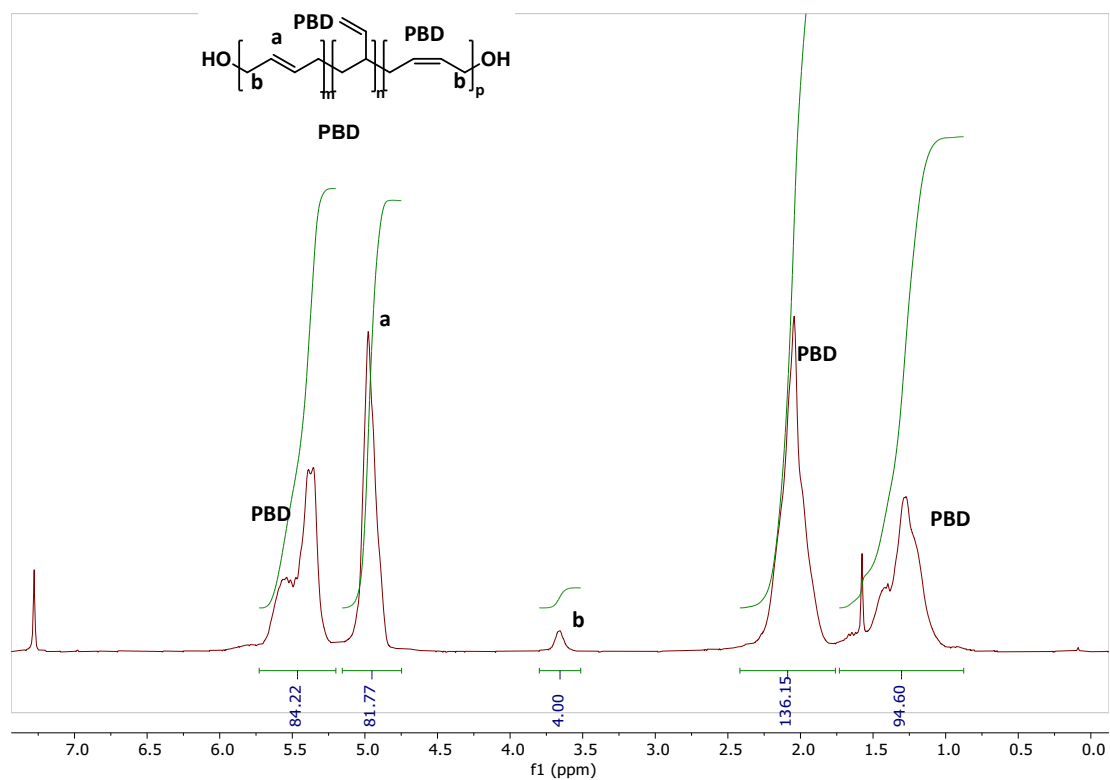


**Figure S24.**  $^1\text{H}$  NMR spectrum ( $\text{CDCl}_3$ , 300 MHz) of HO-PBD-OH macroinitiator

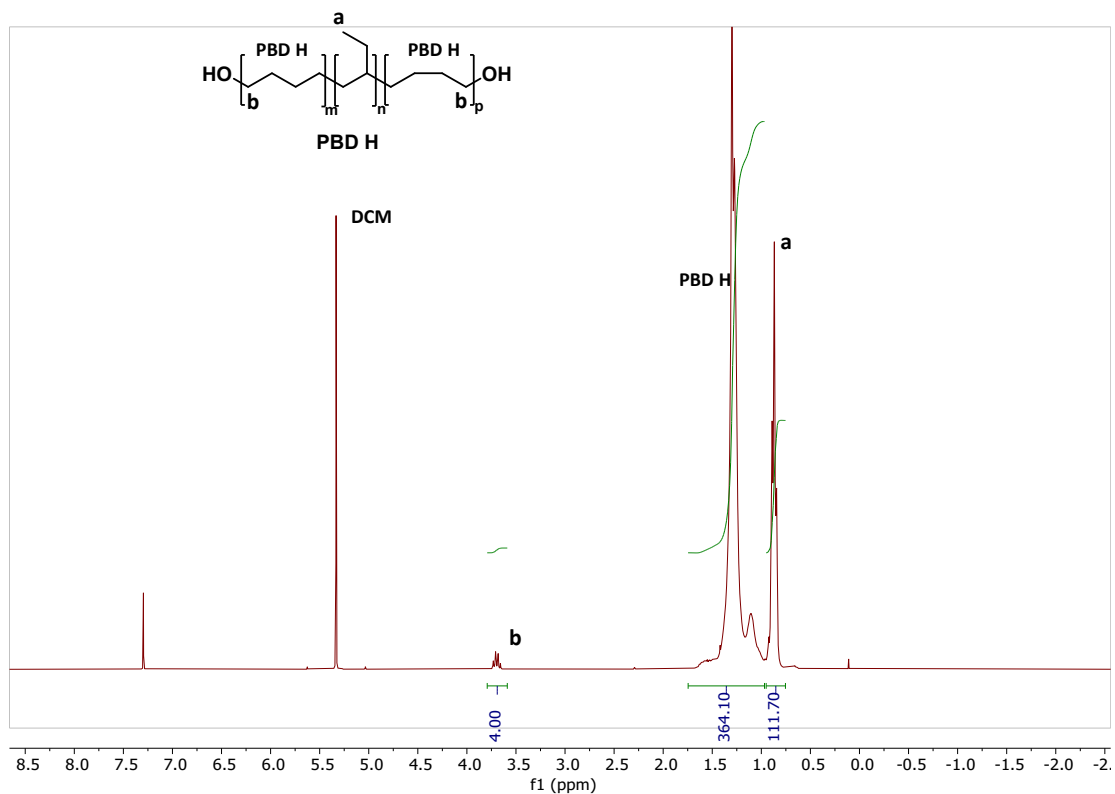


Figure S25.  $^1\text{H}$  NMR spectrum ( $\text{CDCl}_3$ , 300 MHz) of HO-PBD H-OH macroinitiator.

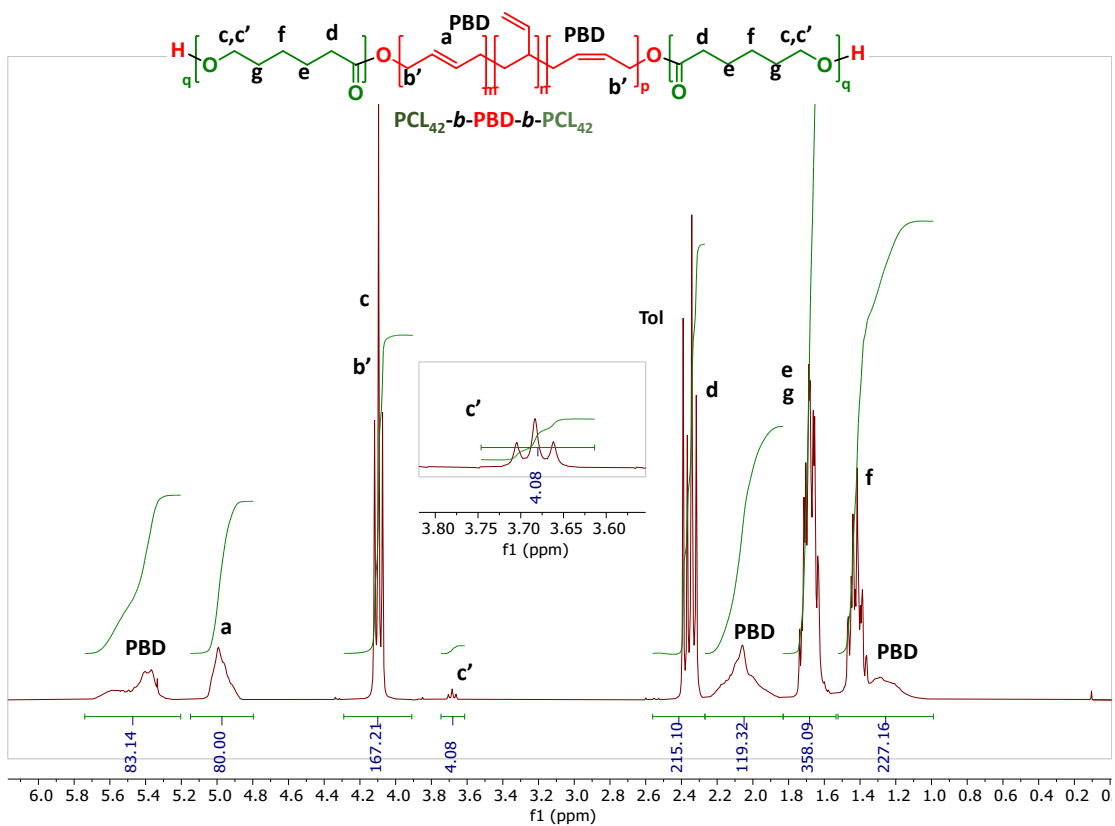
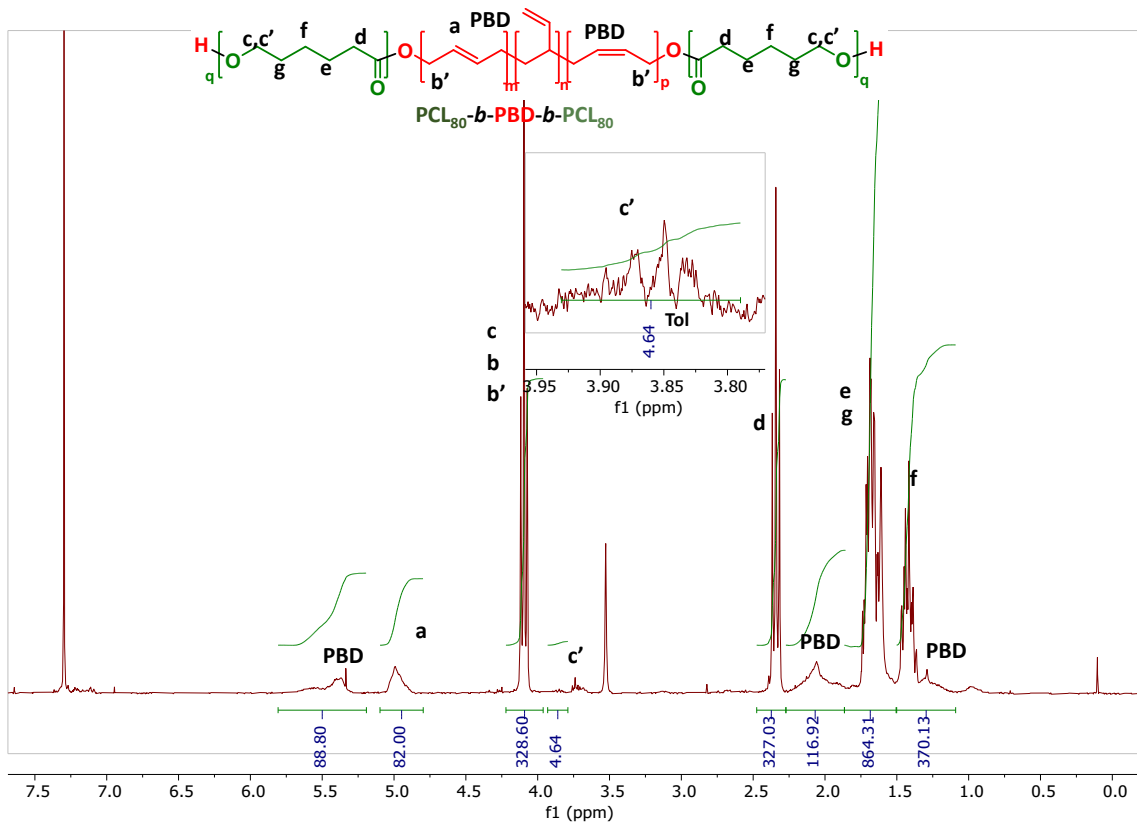
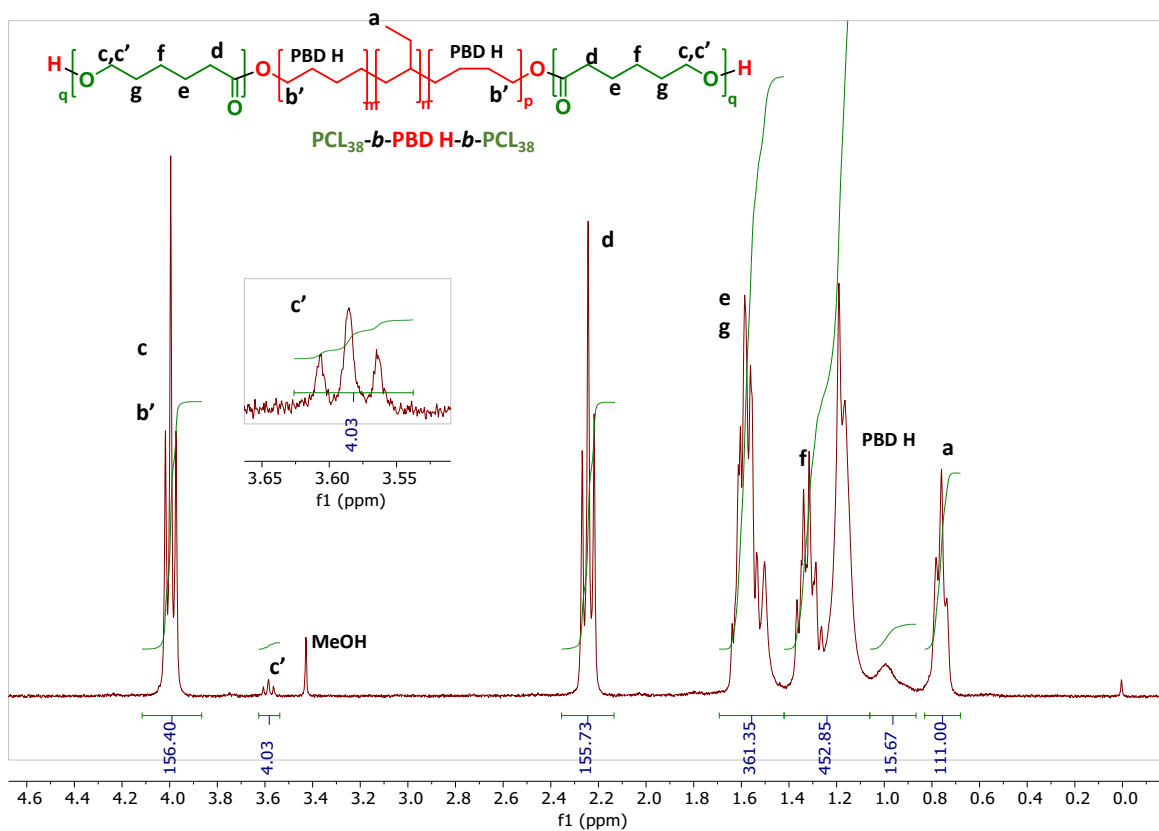


Figure S26.  $^1\text{H}$  NMR spectrum ( $\text{CDCl}_3$ , 300 MHz) of copolymer  $\text{PCL}_{42}$ -*b*-PBD-*b*- $\text{PCL}_{42}$ .



**Figure S27.** <sup>1</sup>H NMR spectrum (CDCl<sub>3</sub>, 300 MHz) of copolymer PCL<sub>80</sub>-*b*-PBD-*b*-PCL<sub>80</sub>



**Figure S28.** <sup>1</sup>H NMR spectrum (CDCl<sub>3</sub>, 300 MHz) of copolymer PCL<sub>38</sub>-*b*-PBD H-*b*-PCL<sub>38</sub>

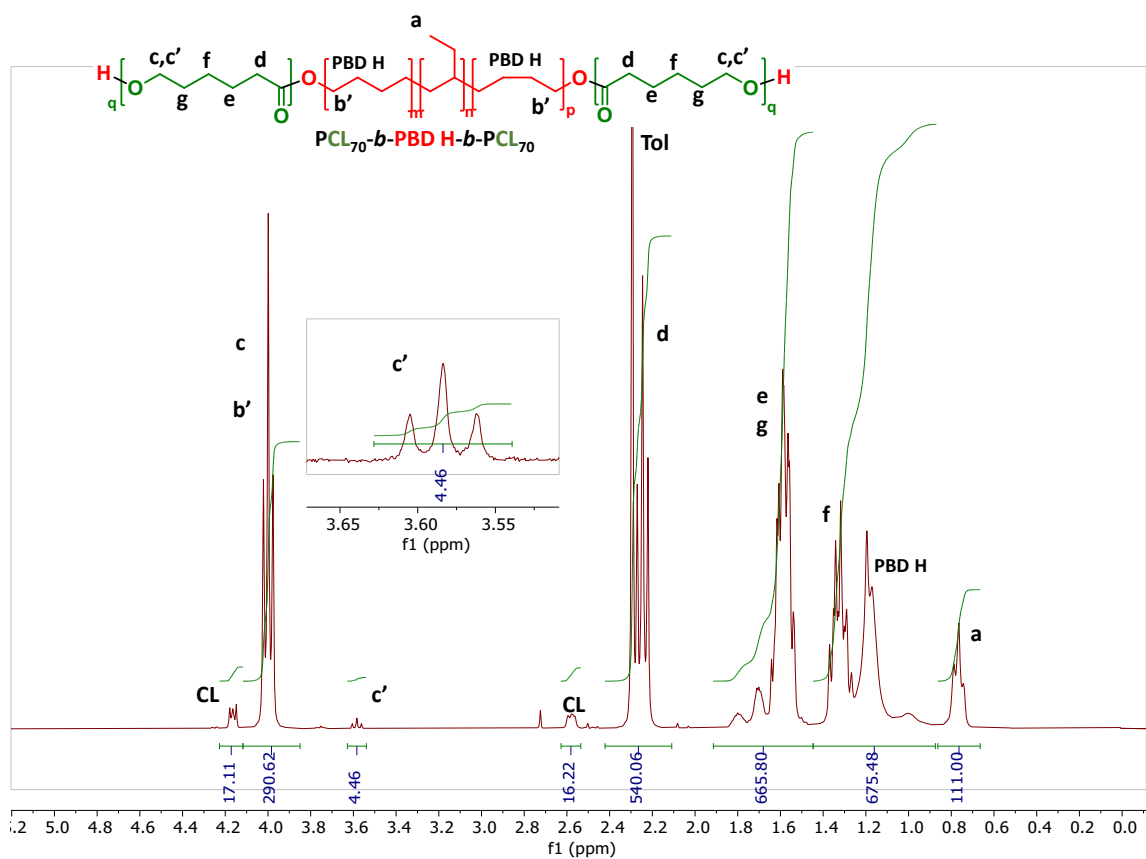


Figure S29.  $^1\text{H}$  NMR spectrum ( $\text{CDCl}_3$ , 300 MHz) of copolymer  $\text{PCL}_{70}\text{-}b\text{-PBD H-}b\text{-PCL}_{70}$

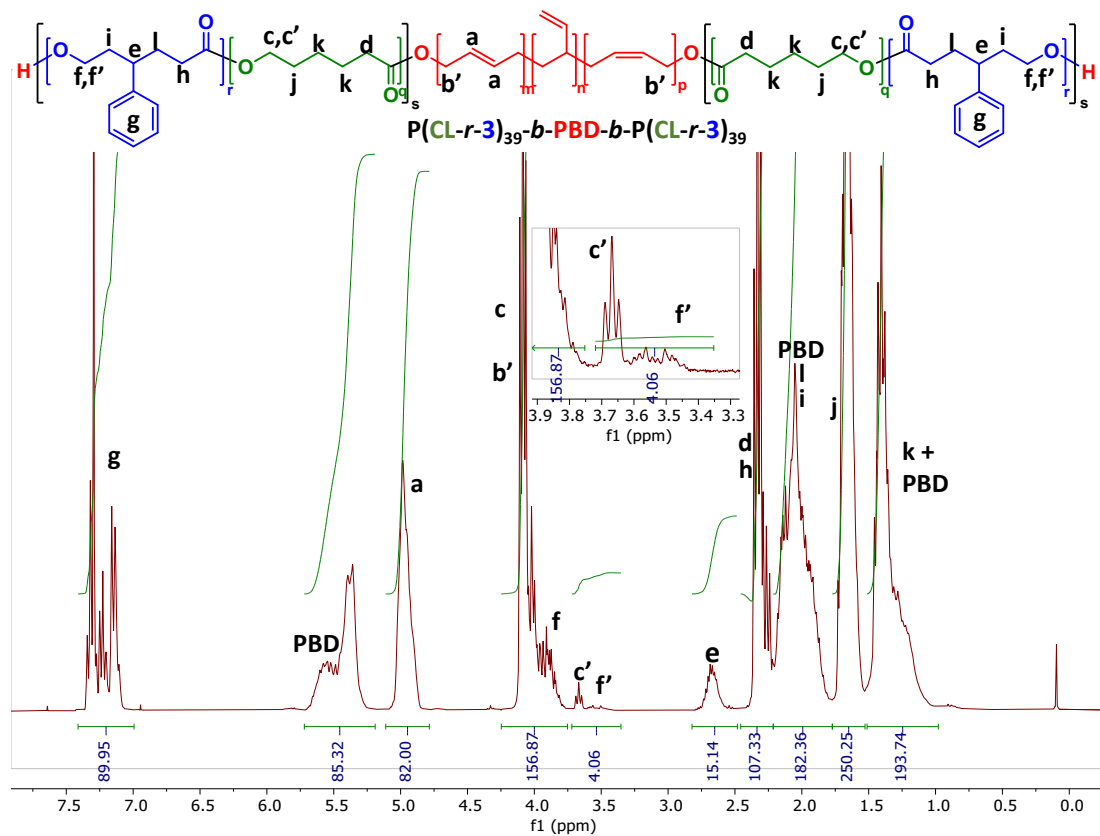


Figure S30.  $^1\text{H}$  NMR spectrum ( $\text{CDCl}_3$ , 300 MHz) of copolymer  $\text{PCL}_{39}\text{-}b\text{-PBD-}b\text{-PCL}_{39}$

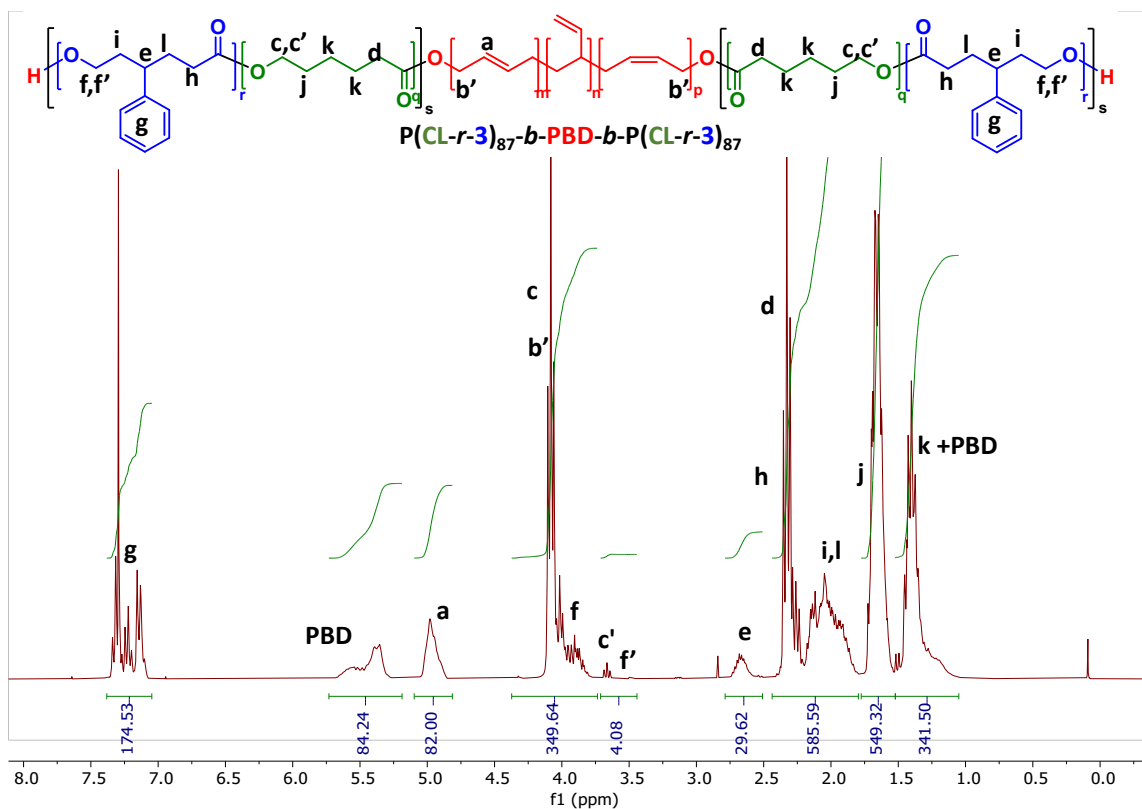


Figure S31. <sup>1</sup>H NMR spectrum (CDCl<sub>3</sub>, 300 MHz) of copolymer PCL<sub>87</sub>-b-PBD-b-PCL<sub>87</sub>

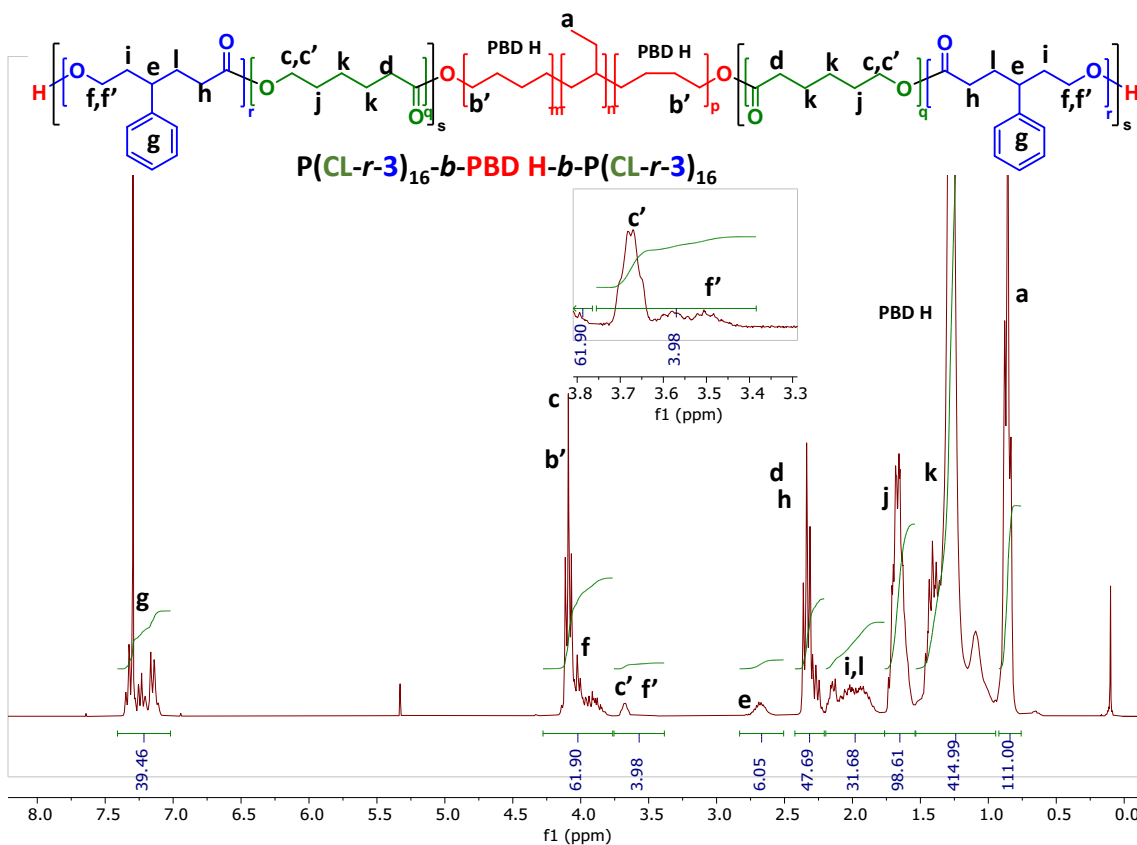


Figure S32. <sup>1</sup>H NMR spectrum (CDCl<sub>3</sub>, 300 MHz) of copolymer PCL<sub>am16</sub>-b-PBD H-b-PCL<sub>am16</sub>

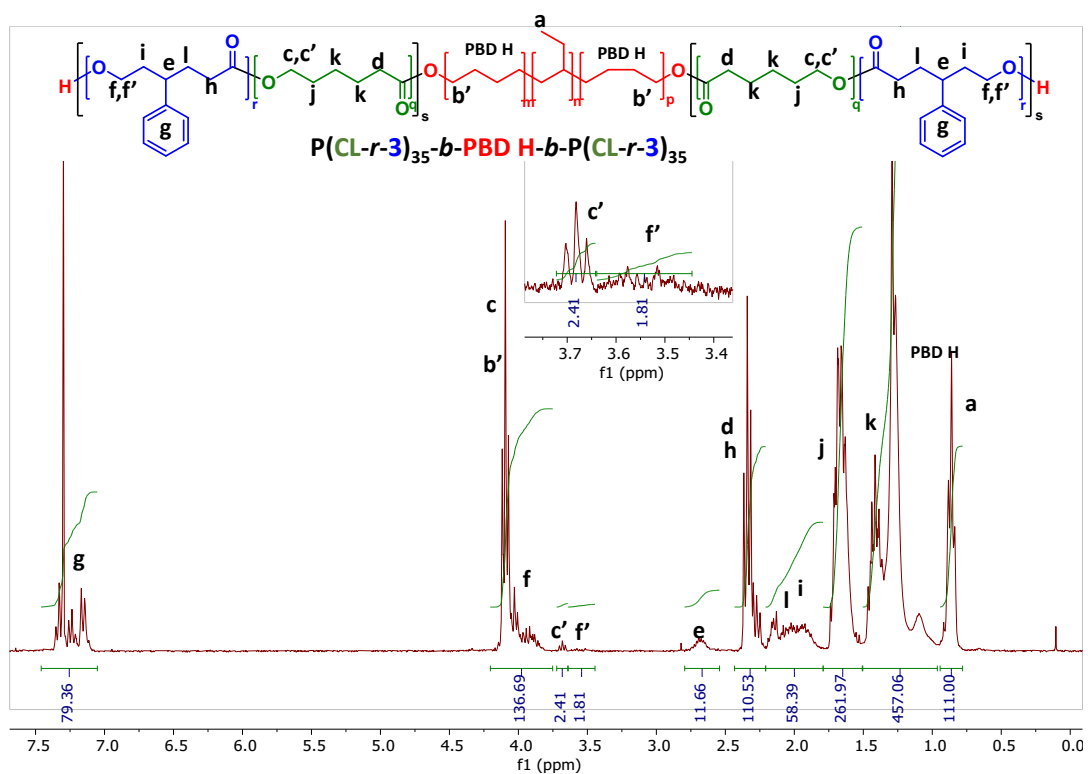


Figure S33.  $^1\text{H}$  NMR spectrum (CDCl<sub>3</sub>, 300 MHz) of copolymer PCL<sub>am35</sub>-b-PBD H-b-PCL<sub>am35</sub>

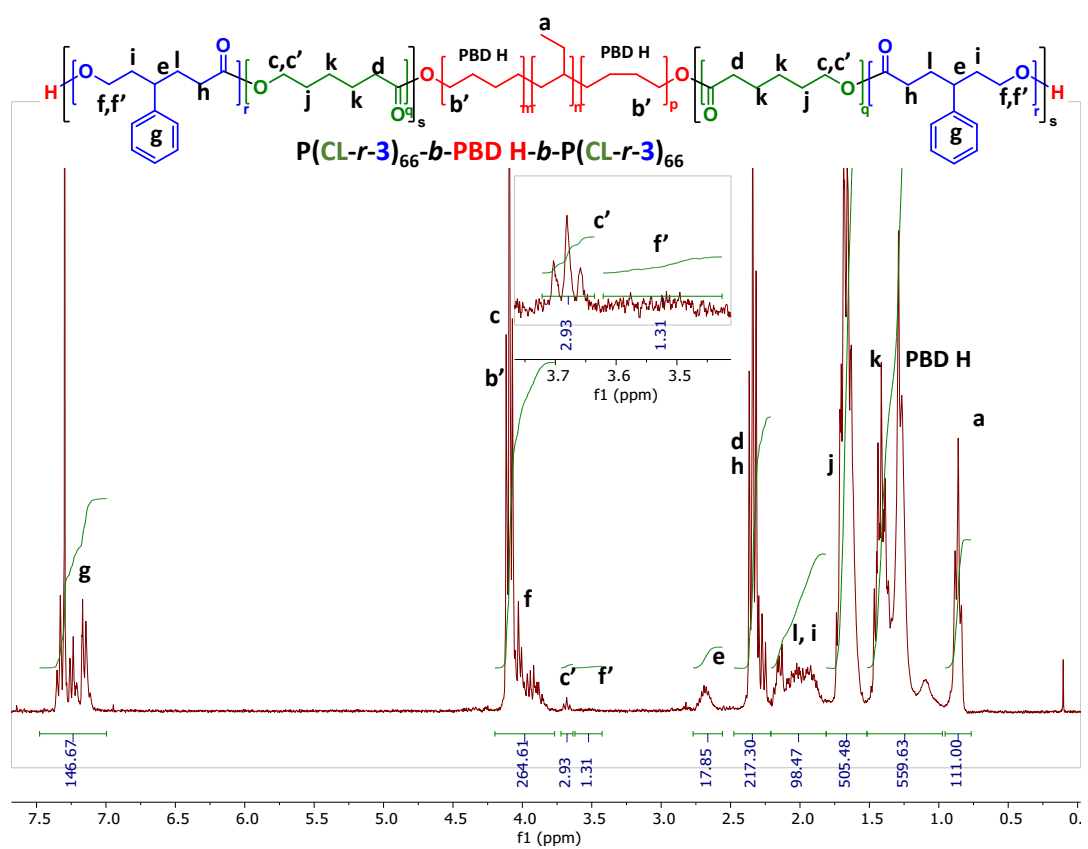
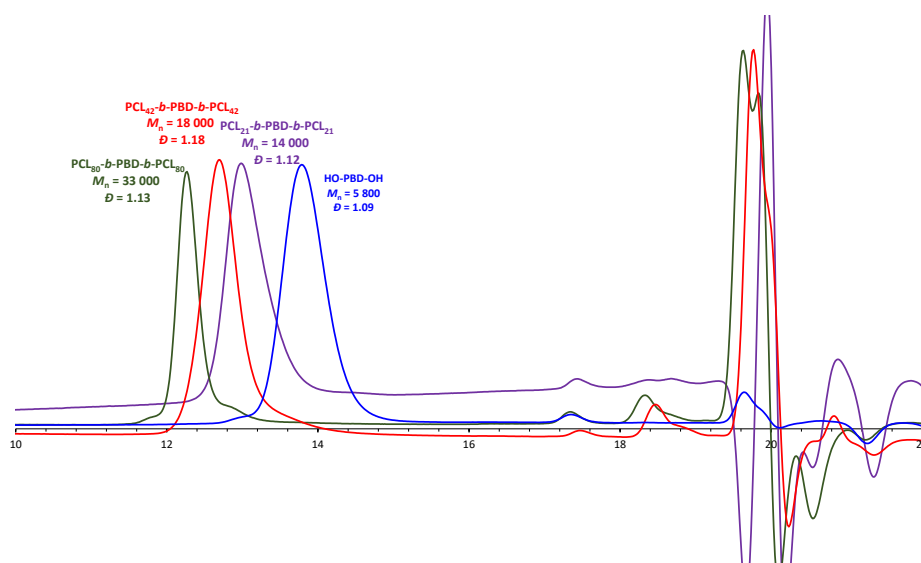
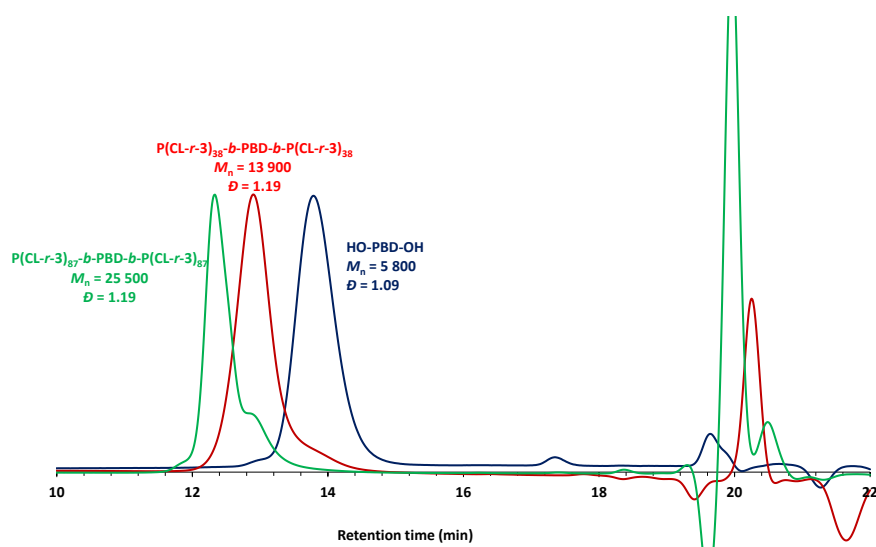


Figure S34.  $^1\text{H}$  NMR spectrum (CDCl<sub>3</sub>, 300 MHz) of copolymer PCL<sub>am66</sub>-b-PBD H-b-PCL<sub>am66</sub>



**Figure S35.** SEC traces of HO-PBD-OH macroinitiator (blue line) and PCL-*b*-PBD-*b*-PCL copolymers (violet, red and green lines).



**Figure S36.** SEC traces of HO-PBD-OH macroinitiator (blue line) and PCL<sub>am</sub>-*b*-PBD-*b*-PCL<sub>am</sub> copolymers (red and green line).



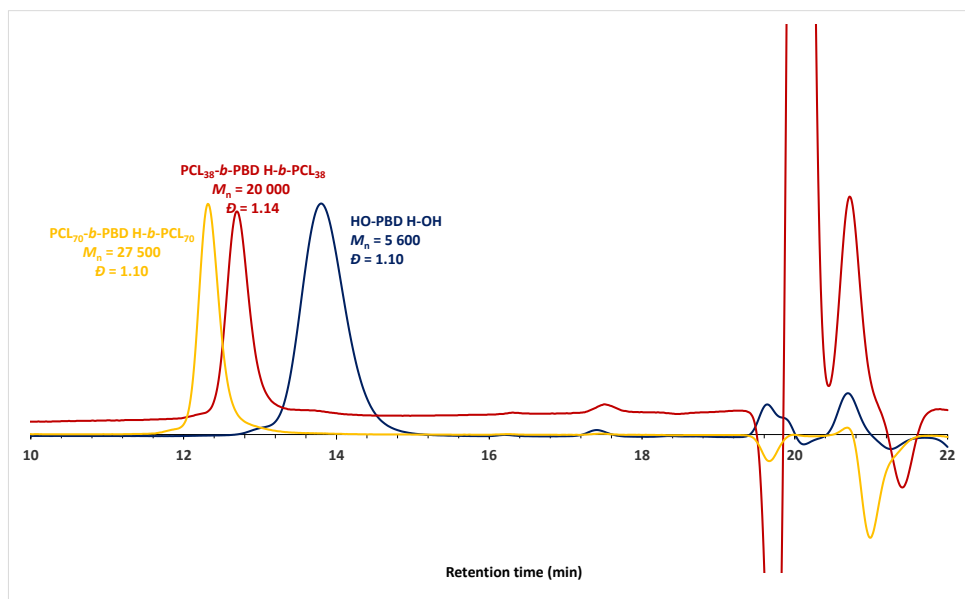


**Figure S37.** SEC traces of HO-PBD H-OH macroinitiator (blue line) and PCL-*b*-PBD-*b*-PCL copolymers (red and orange line).

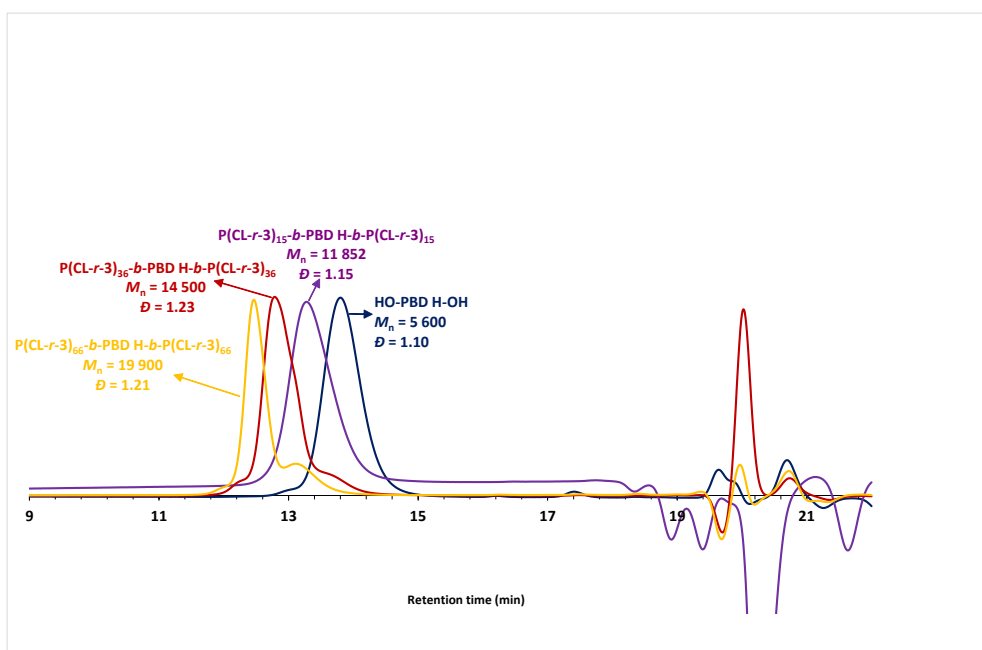


**Figure S38.** SEC traces of HO-PBD H-OH macroinitiator (blue line) and PCL<sub>am</sub>-*b*-PBD-*b*-PCL<sub>am</sub> copolymers (violet, red and orange line).

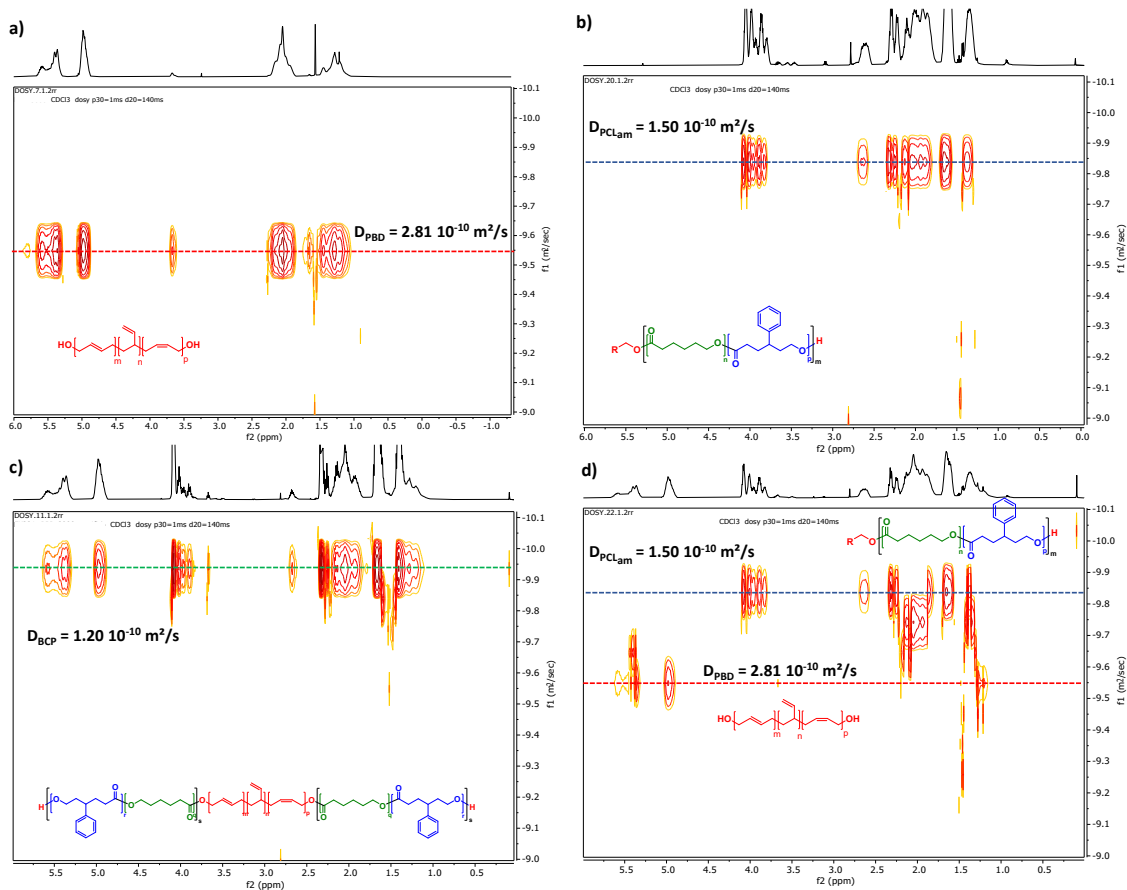


**Figure S39:** 2D DOSY  $^1\text{H}$  spectra ( $\delta = 1 \text{ ms}$  and  $\Delta = 140 \text{ ms}$ ) of  $\text{CDCl}_3$  solution of: (a) PBD macroinitiator; (b) P(CL-*r*-3) of  $M_n = 12\,000 \text{ g/mol}$ ; (c) BCP PCL<sub>am39</sub>-*b*-PBD-*b*-PCL<sub>am39</sub>; (d) Blend of PBD macroinitiator and P(CL-*r*-3)

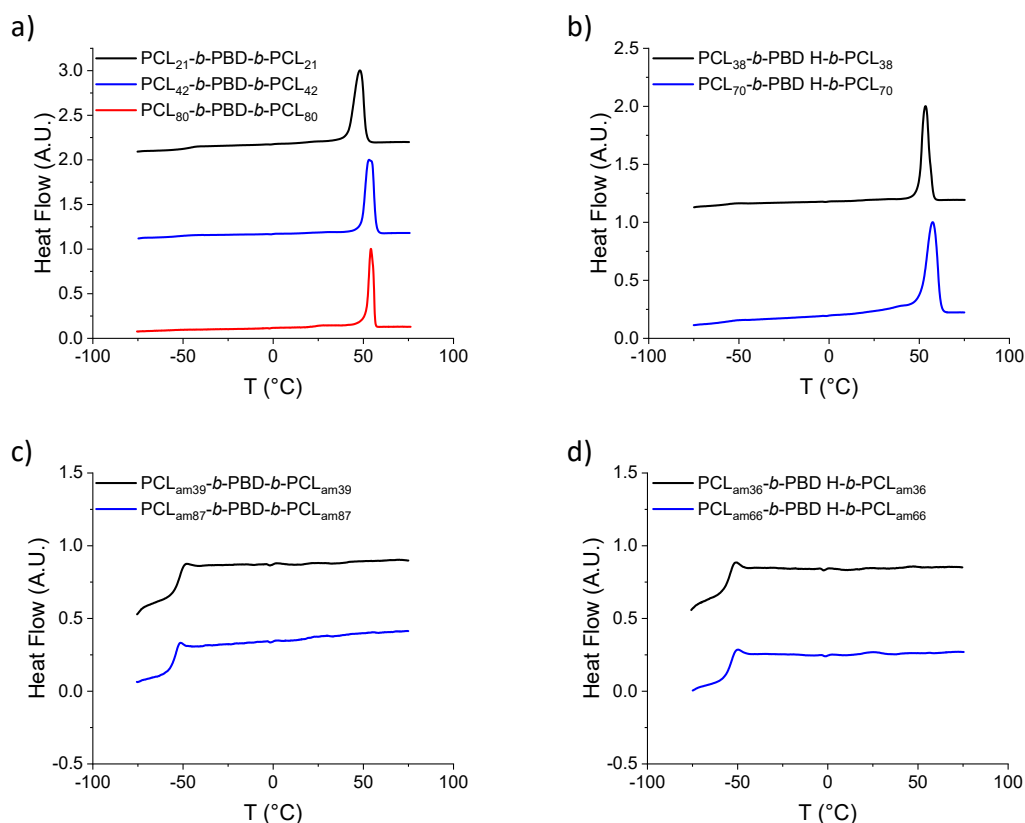


**Figure S40:** DSC traces (endo up) obtained for the 2<sup>nd</sup> heating cycle at 10°C/min for (a) PCL-*b*-PBD-*b*-PCL and (b) PCL-*b*-PBD H-*b*-PCL, (c) PCL<sub>am</sub>-*b*-PBD-*b*-PCL<sub>am</sub> and (d) PCL<sub>am</sub>-*b*-PBD H-*b*-PCL<sub>am</sub> triblock copolymers. The curves have been shifted and normalized for clarity.

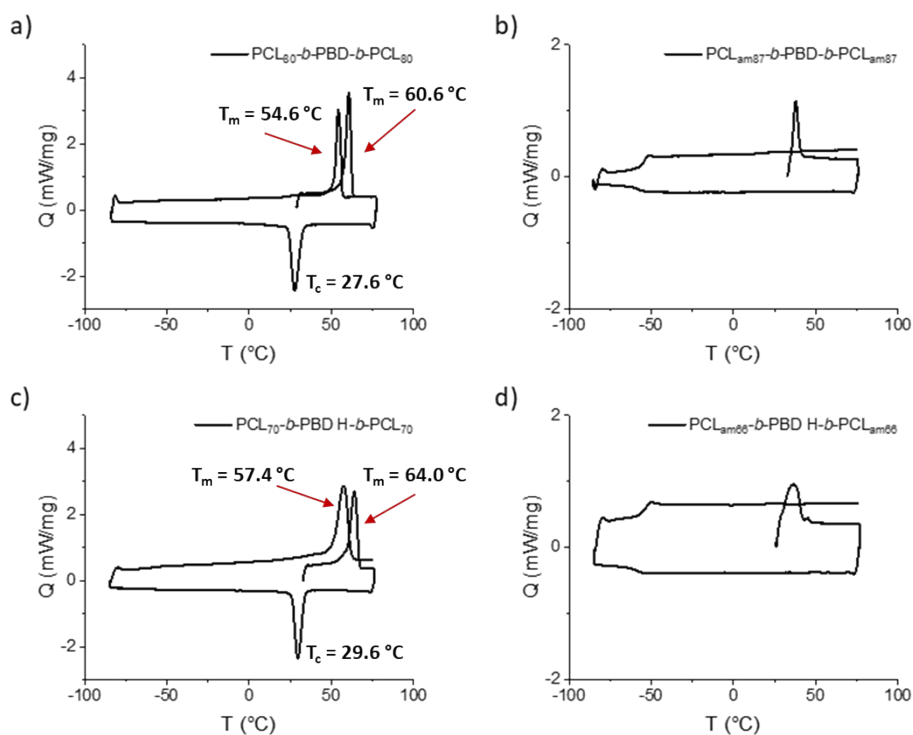


**Figure S41.** Full DSC traces (endo up) obtained at 10°C/min for (a) PCL<sub>80</sub>-*b*-PBD-*b*-PCL<sub>80</sub> and (b), PCL<sub>am87</sub>-*b*-PBD-*b*-PCL<sub>am87</sub>, (c) PCL<sub>70</sub>-*b*-PBD H-*b*-PCL<sub>70</sub> and (d) PCL<sub>am66</sub>-*b*-PBD H-*b*-PCL<sub>am66</sub> triblock copolymers.

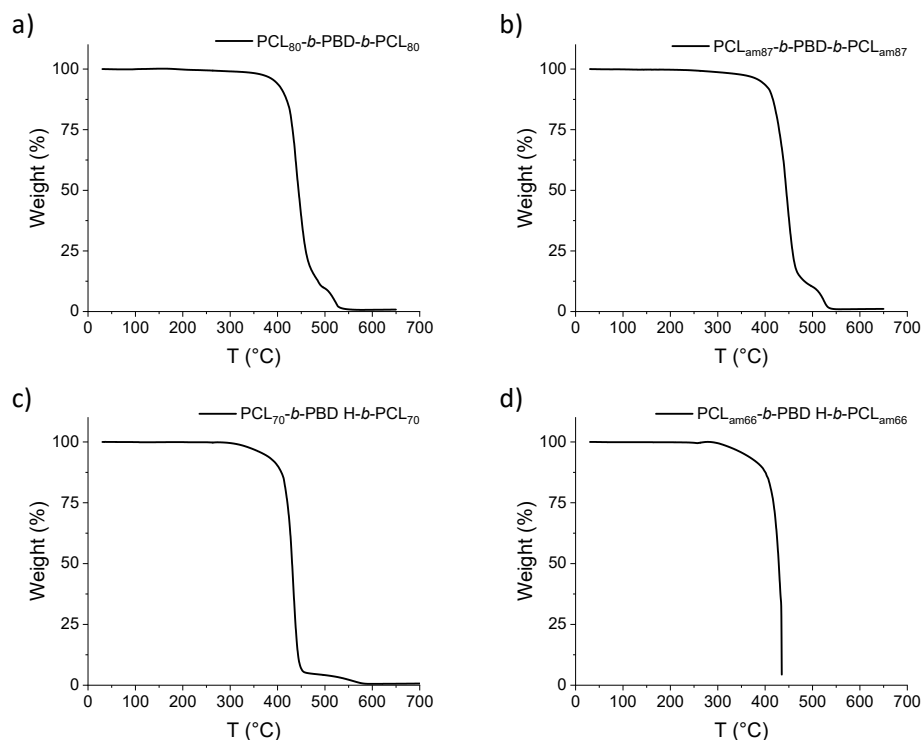


**Figure S42.** TGA traces obtained for selected triblock copolymers: (a)  $\text{PCL}_{80}\text{-}b\text{-PBD-}b\text{-PCL}_{80}$ ,  $T_d = 371$  °C; (b)  $\text{PCL}_{\text{am}87}\text{-}b\text{-PBD-}b\text{-PCL}_{\text{am}87}$ ,  $T_d = 367$  °C; (c)  $\text{PCL}_{70}\text{-}b\text{-PBD H-}b\text{-PCL}_{70}$ ,  $T_d = 350$  °C; (d)  $\text{PCL}_{\text{am}66}\text{-}b\text{-PBD H-}b\text{-PCL}_{\text{am}66}$ ,  $T_d = 333$  °C.

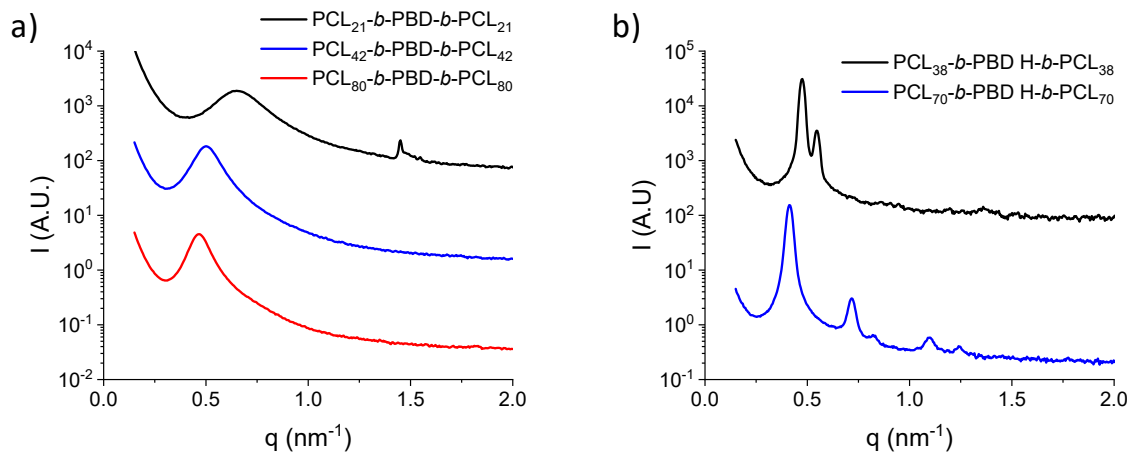


**Figure S43.** (a) SAXS spectra of  $\text{PCL-}b\text{-PBD-}b\text{-PCL}$  and (b)  $\text{PCL-}b\text{-PBD H-}b\text{-PCL}$  block copolymers acquired at 100°C.

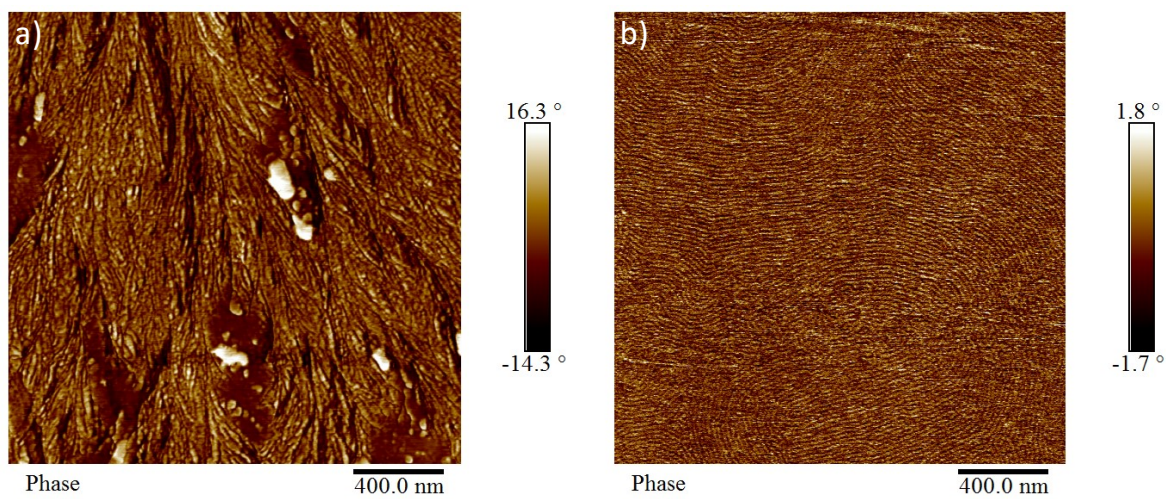


**Figure S44.** ( $2\ \mu\text{m} \times 2\ \mu\text{m}$ ) AFM phase images of phase-separated structures obtained for (a)  $\text{PCL}_{70}\text{-}b\text{-PBD H-}b\text{-PCL}_{70}$  and (b)  $\text{PCL}_{\text{am}66}\text{-}b\text{-PBD H-}b\text{-PCL}_{\text{am}66}$ .